N/Z Equilibration in Binary Nuclear Systems

R.T. deSouza
Indiana University

Special Thanks: K. Brown, A.B. McIntosh, **S. Hudan**

Using isospin transport to learn about the symmetry energy

Neutron star merger

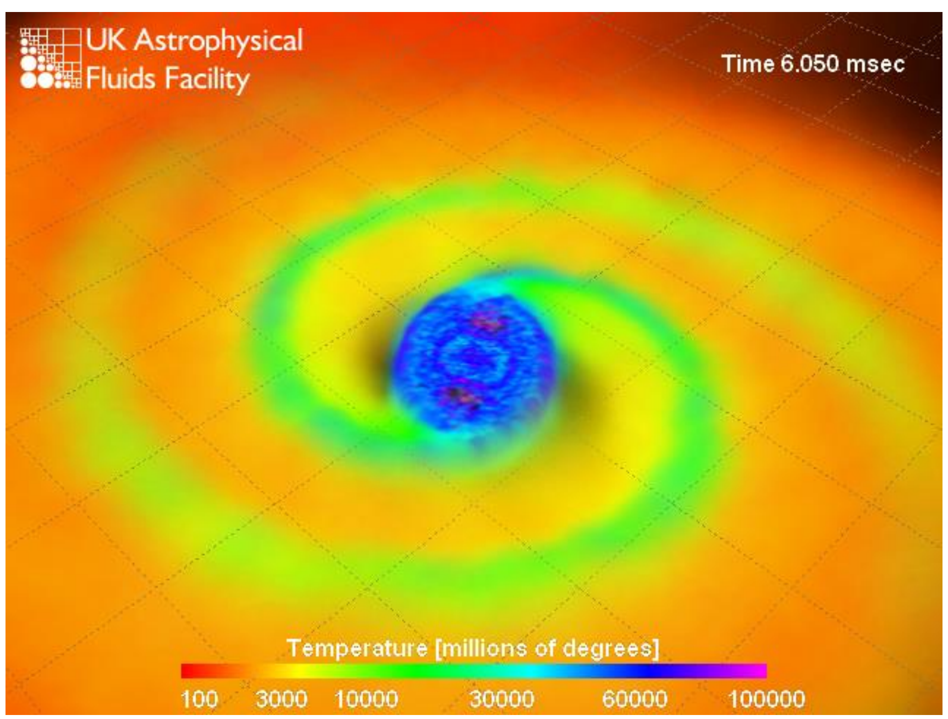

Heavy-ion collisions

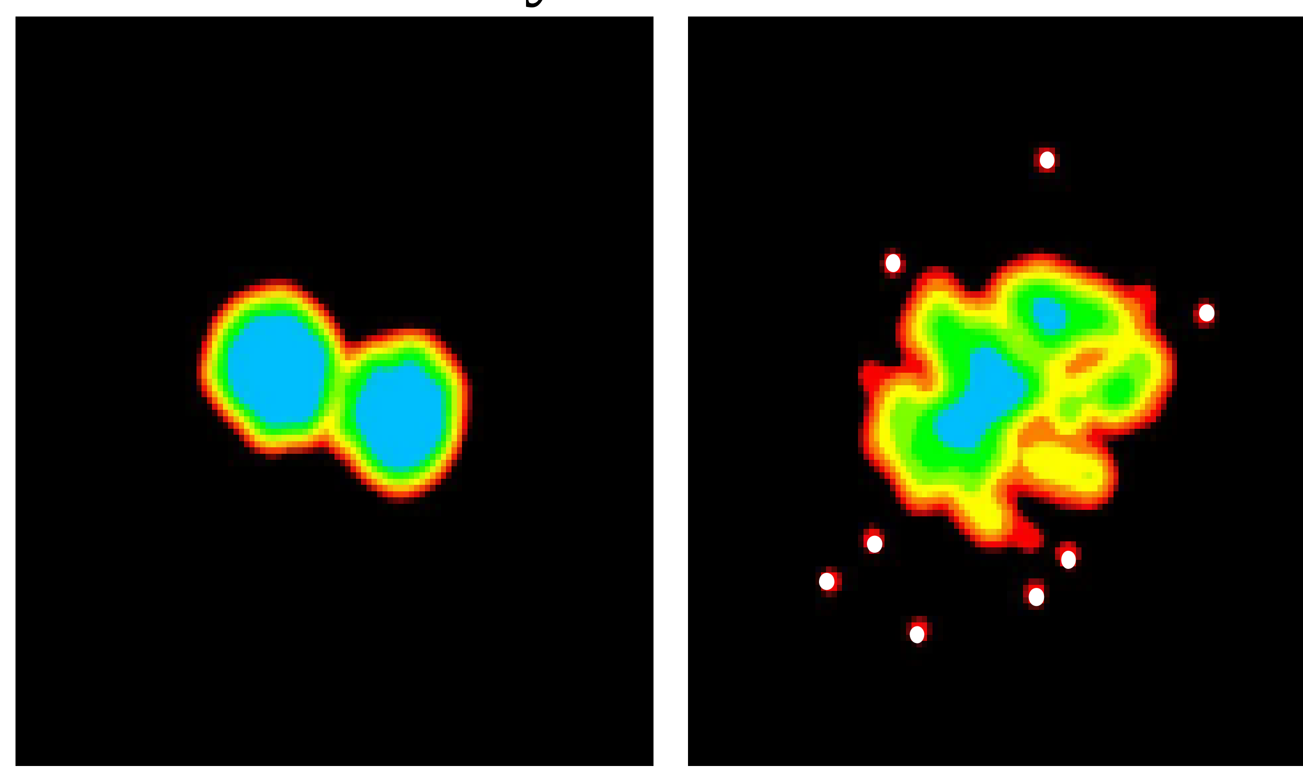

Work supported by the US Dept. of Energy under Grant No. DEFG02-88ER-40404

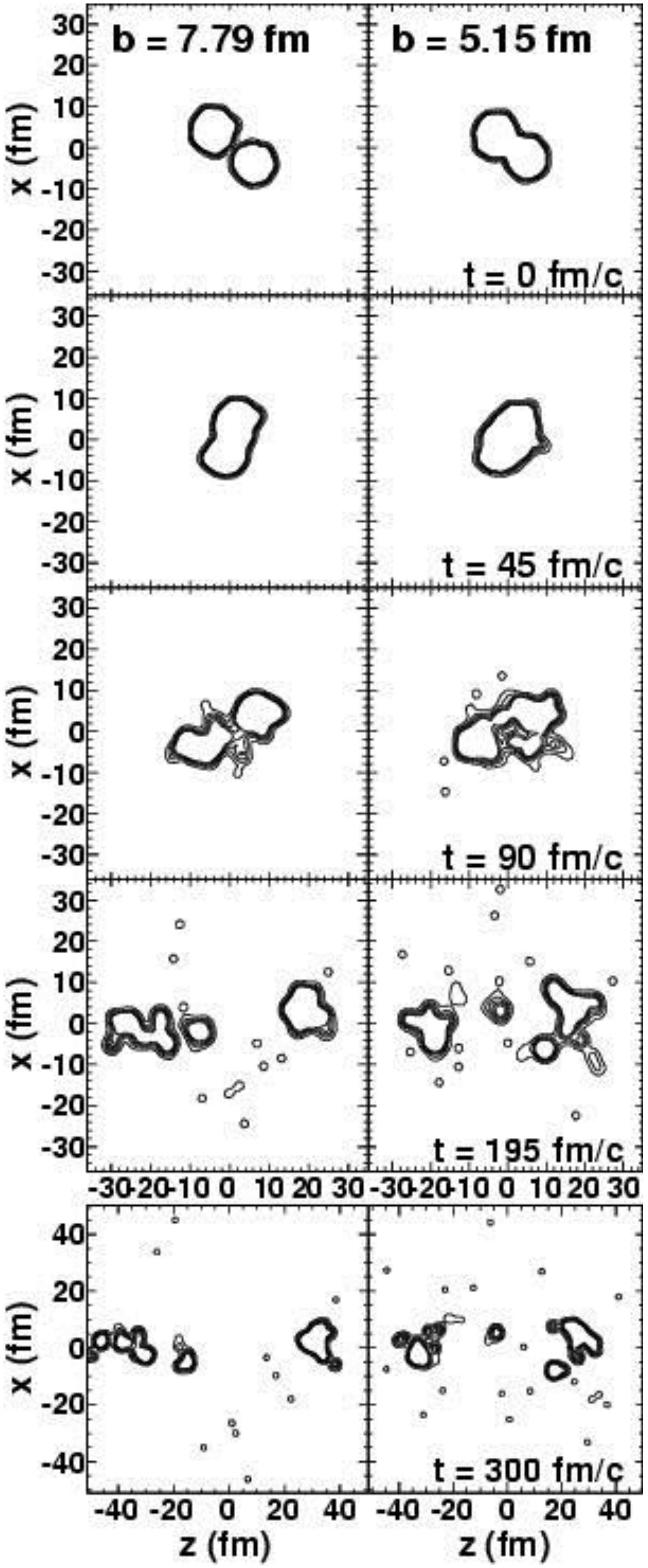

AMD: A microscopic picture

- System:
  ^{114}Cd + ^{92}Mo at 50 MeV/nucleon

☞ Mass, charge, energy exchange

☞ Binary nature of the collision

☞ **Transiently deformed nuclei**

☞ Early cluster production, t ≈ 90 fm/c

Clusters are also statistically emitted as the excited reaction products de-excite!

S.Hudan, R.T. de Souza and A. Ono, PRC (2005)

Isospin Transport: Drift and Diffusion

$$j_{p/n} = \boxed{D^{\rho}_{p/n}\nabla\rho} - \boxed{D^{I}_{p/n}\nabla I}$$

Drift

Diffusion

$$\rho = \rho_n + \rho_p$$

$$I = \frac{\rho_n - \rho_p}{\rho}$$

$$D^{\rho}_{n} - D^{\rho}_{p} \propto 4I\frac{\partial E_{sym}}{\partial \rho}$$

$$D^{I}_{n} - D^{I}_{p} \propto 4\rho E_{sym}$$

- **Isospin Drift**: due to density gradients
  - Migration of neutrons to low-density region
  - Slope of the symmetry energy

Baran, PRC72, 064620 (2005)
Rizzo, NPA806, 79 (2008)

- **Isospin Diffusion**: due to N/Z gradients
  - Migration of neutrons from high N/Z region to low N/Z region
  - Absolute value of the symmetry energy

N/Z Asymmetric Collisions

- Overlapping Fermi tails / low density neck→ drift
- Initial N/Z asymmetry → diffusion
- Probe: Isotopic composition of emitted clusters

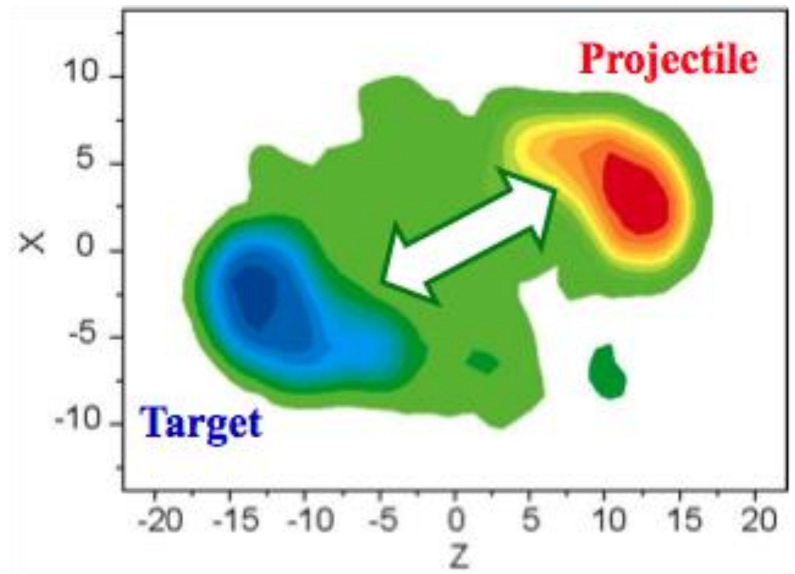

Liu, PRC76, 034603 (2007)
Kohley, PRC 85, 064605 (2012)
Barlini, PRC87, 054607 (2013)
…

Ratios (R_X): Use cross-bombardment of n-rich and n-poor nuclei to reduce common characteristics (e.g. drift) to first order

Rami, PRL84, 1120 (2000)

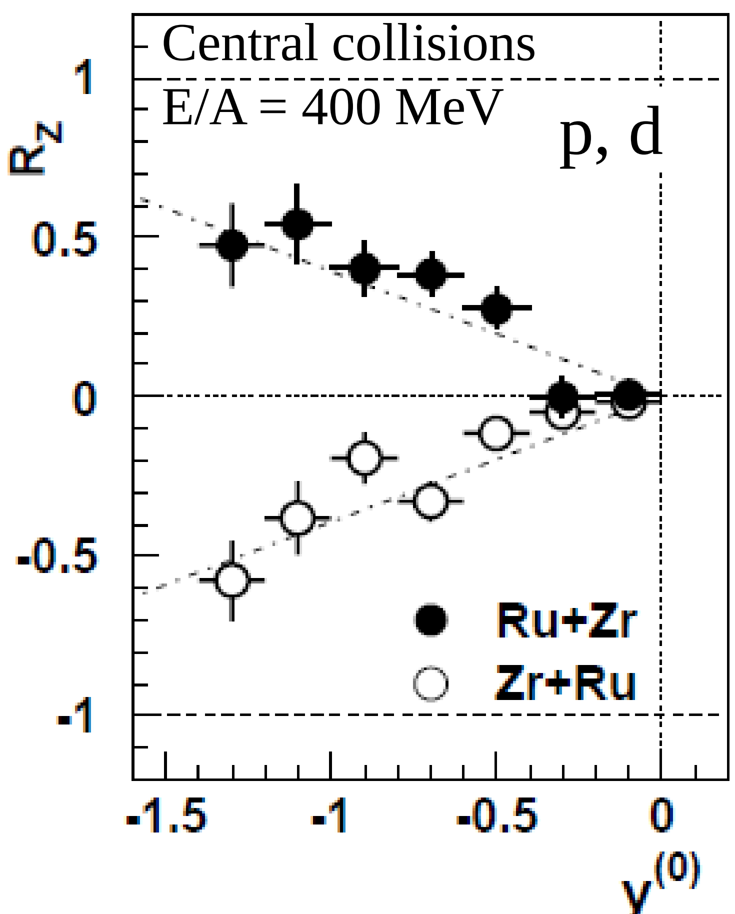

Tsang, PRL92, 062701 (2004)

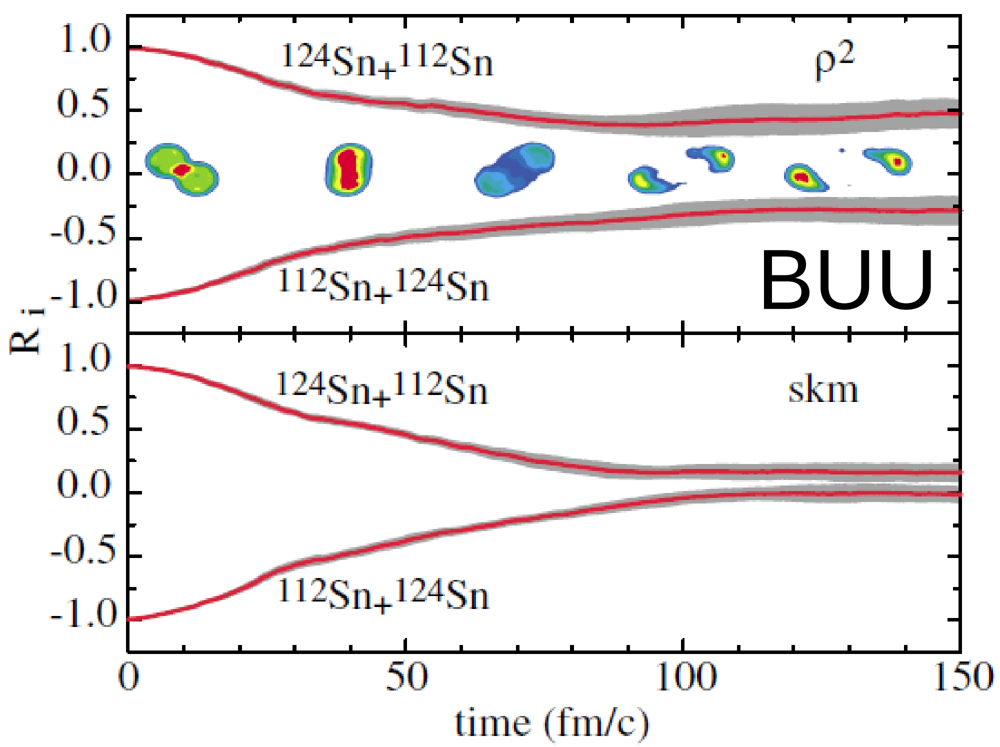

±1: no equilibration
0: equilibration

- Observed degree of equilibration limited by the **short** contact **time** between the target and the projectile (~100 fm/c).

Experimental Setup

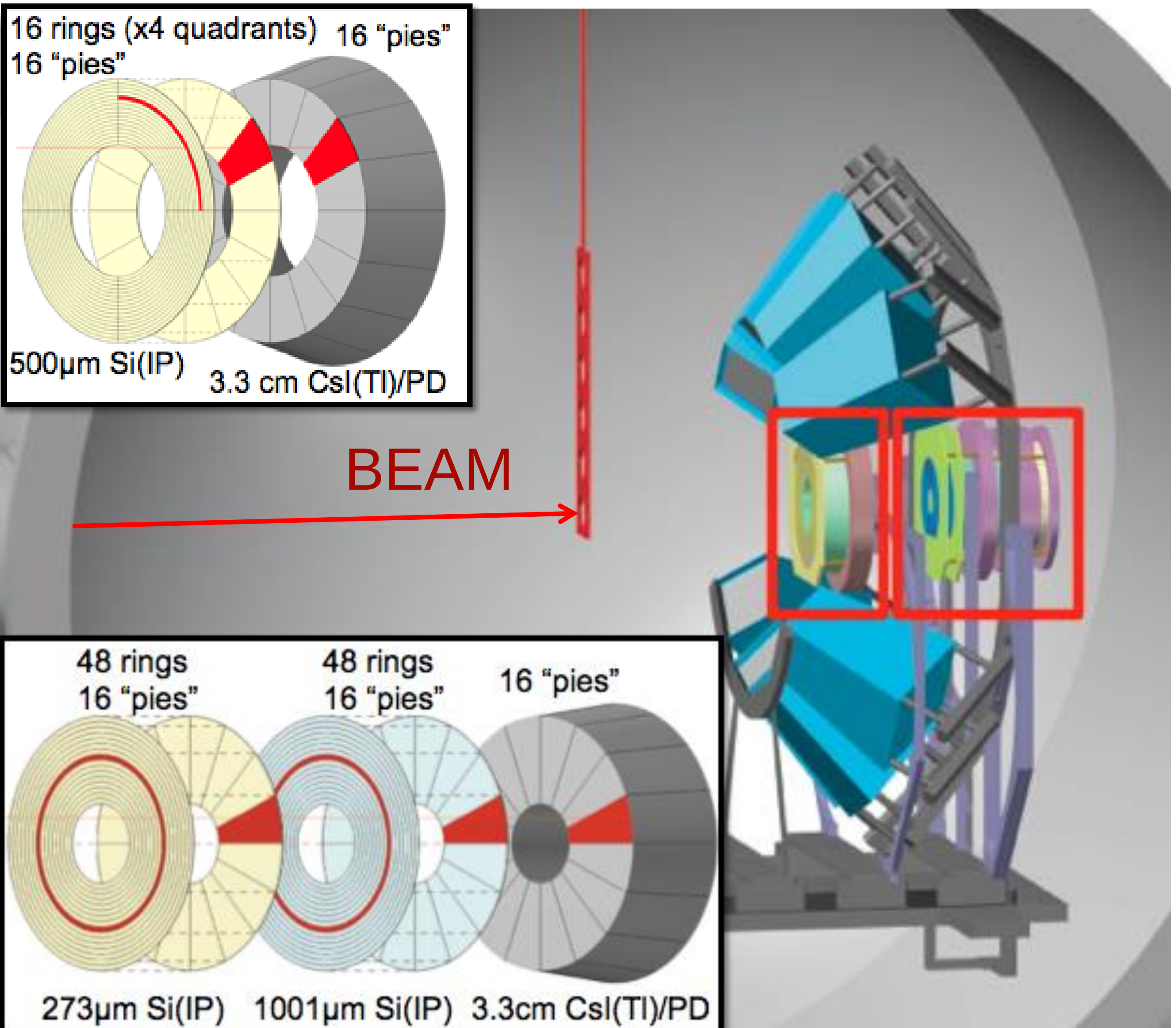

Forward Indiana Ring Silicon Telescope

Large Area Silicon Strip Array

FIRST: T. Paduszynski *et. al.*, NIM A **547**, 464 (2005)
LASSA: B. Davin *et. al.*, NIM A **473**, 302 (2001)
A. Wagner *et. Al.*, NIM A **456**, 209 (2001)

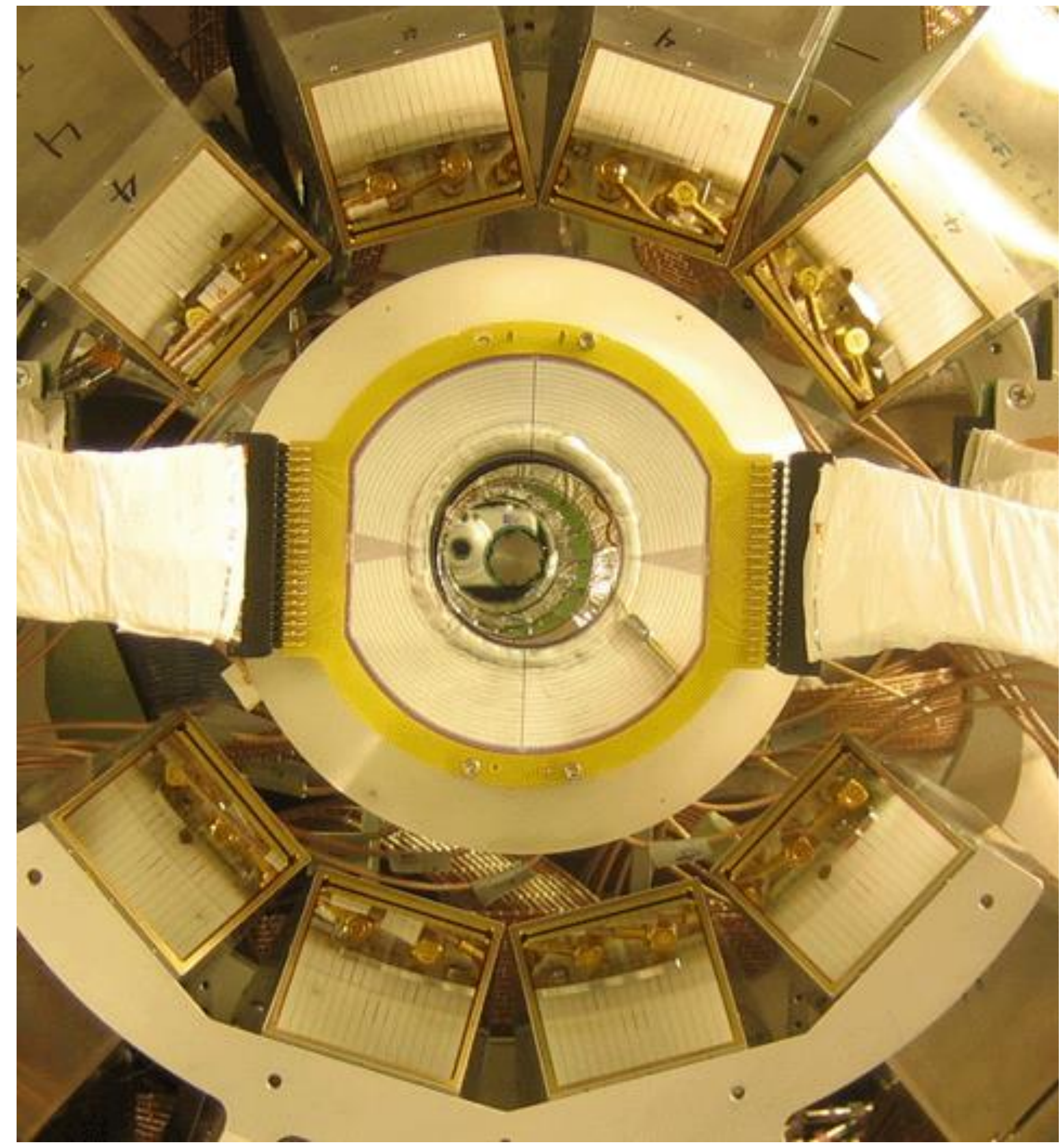

Si-CsI stack detectors &
Si-Si-CsI stack detectors
→ **ΔE-E technique**

High Segmentation → High Angular Resolution
(592 Si channels)

Angular coverage: $3° \leq \theta_{Lab} \leq 51°$ (FIRST+LASSA)

Systems Investigated

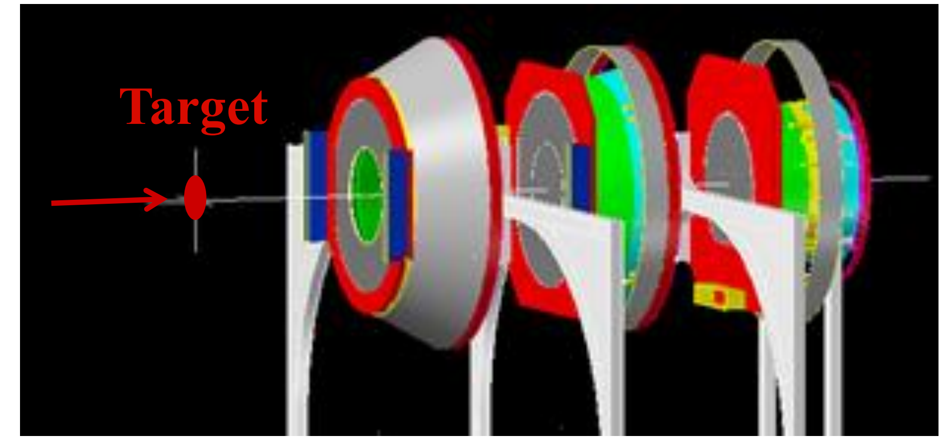

Paduszynski, NIMA547, 464 (2005)

- :
  - ^{124}Xe + ^{112,124}Sn @ 49 MeV/A (GANIL)
  - ^{64}Zn + ^{64}Zn, ^{209}Bi, ^{27}Al @ 45 MeV/A (TAMU)
- Experimental Setup:
  - Angular coverage: 3° ≤ θ_{Lab} ≤ 28° (FIRST)
  - Z and A identification by ΔE-E
  - A identification up to Z = 14

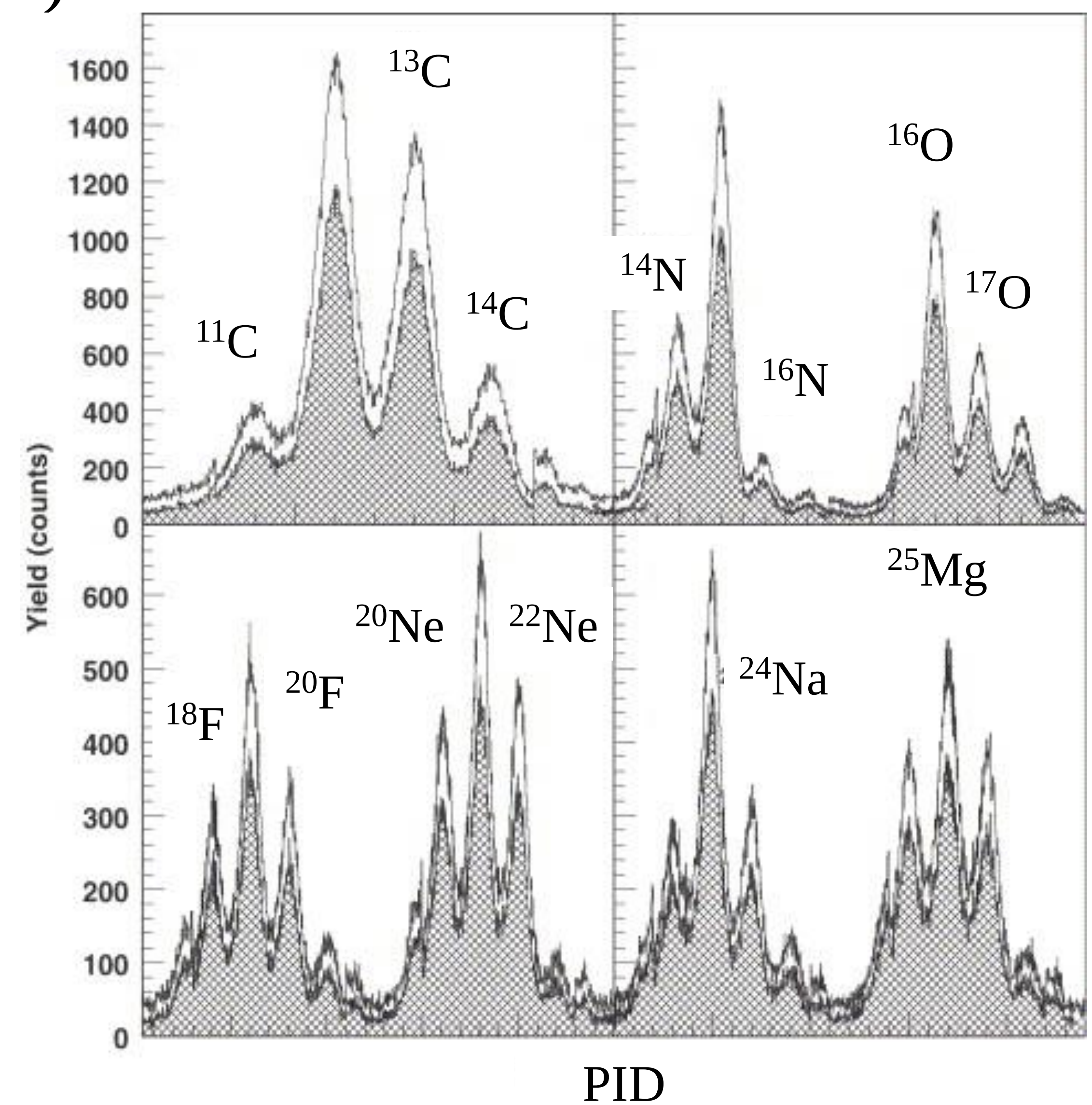

Energy calibration of FIRST (T1)

Silicon detectors

^{13}C Beam Calibration

→ Silicon Detector Thickness

Charge Pulser Calibration

→ Establish Linearity of Electronics

Isotope lines of known Z,A

& Energy Loss Calculations

→ Silicon Detector Energy Calibration

CsI detector calibration

Isotopic lines of known Z,A

& Silicon detector calibration

& Energy Loss Calculations

→ CsI Energy Calibration

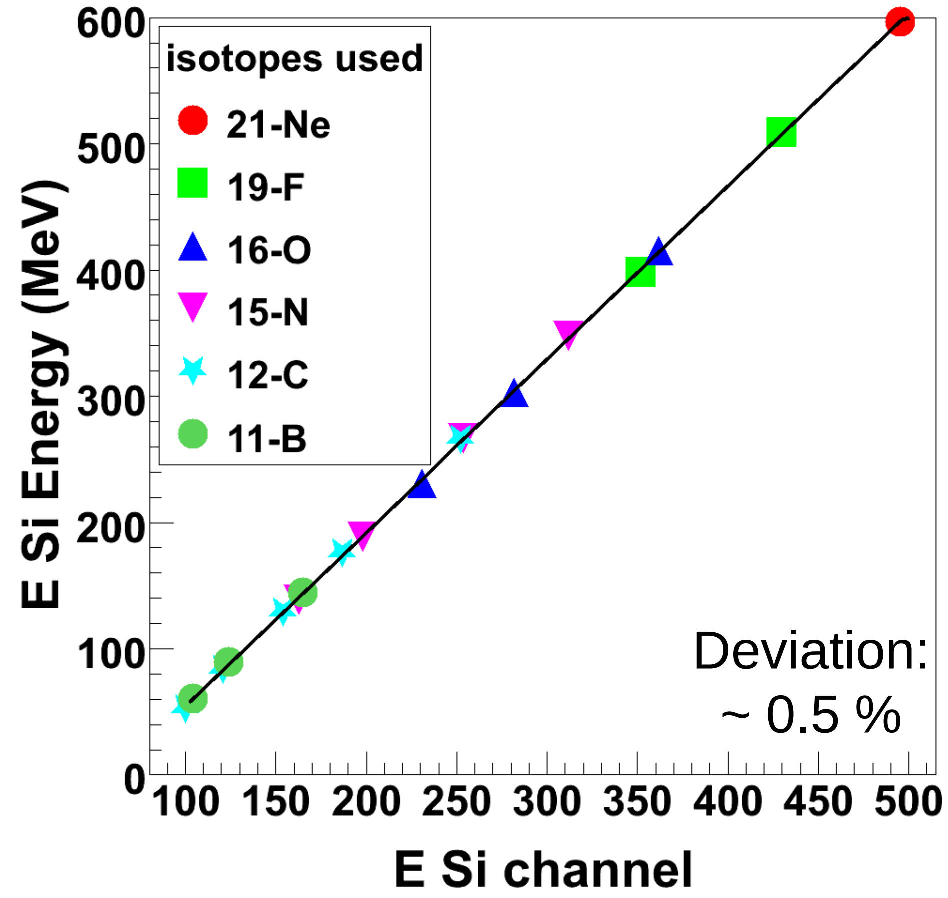

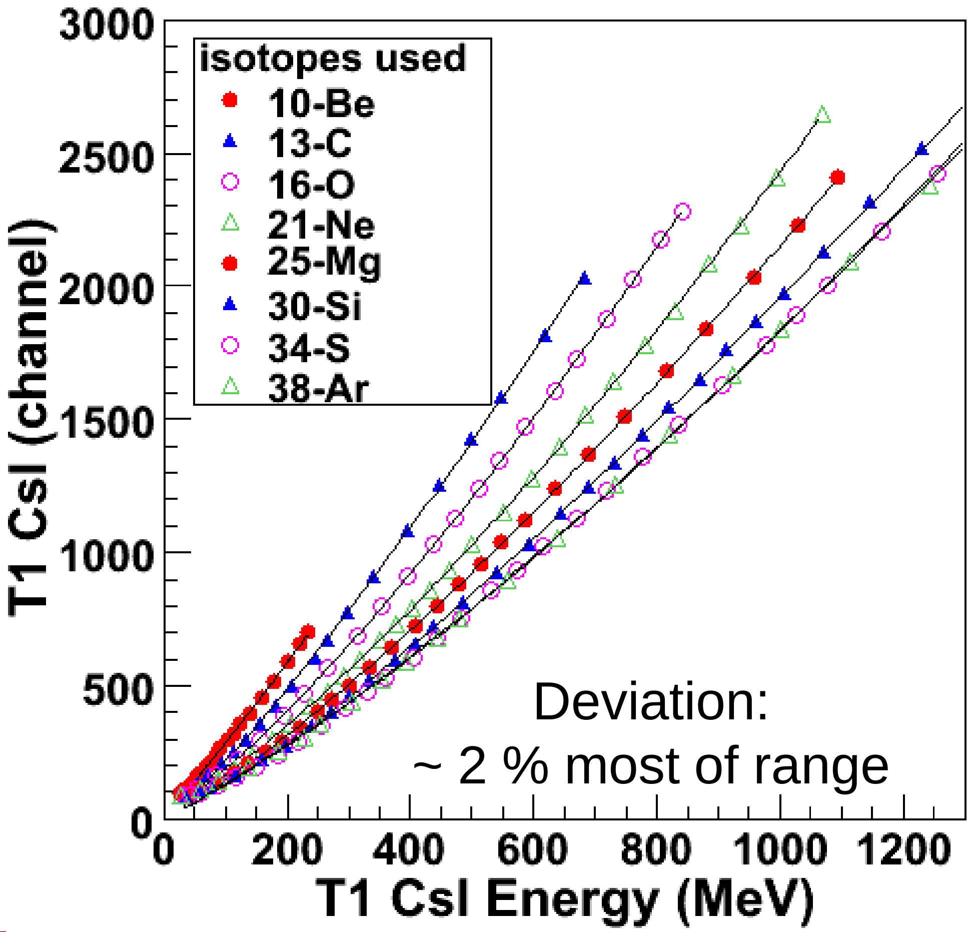

Projectile-Like Fragment (PLF)

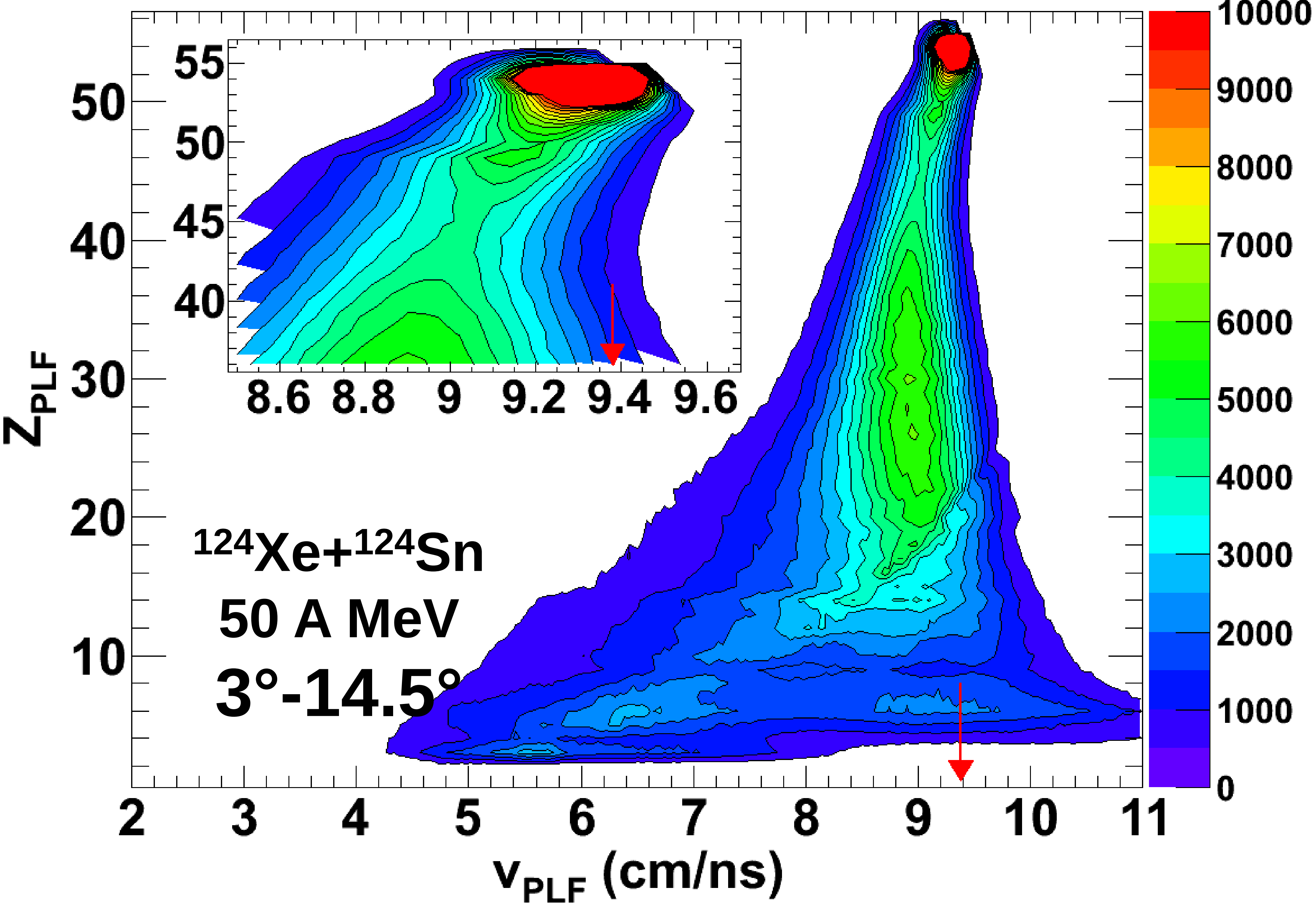

PLF

Heaviest particle detected in FIRST (3°-14°)

- As Z decreases from Z_{beam}, velocity initially decreases (damping)
- As Z continues to decrease, velocity remains "about" constant (apparent saturation of damping)

Velocity of PLF

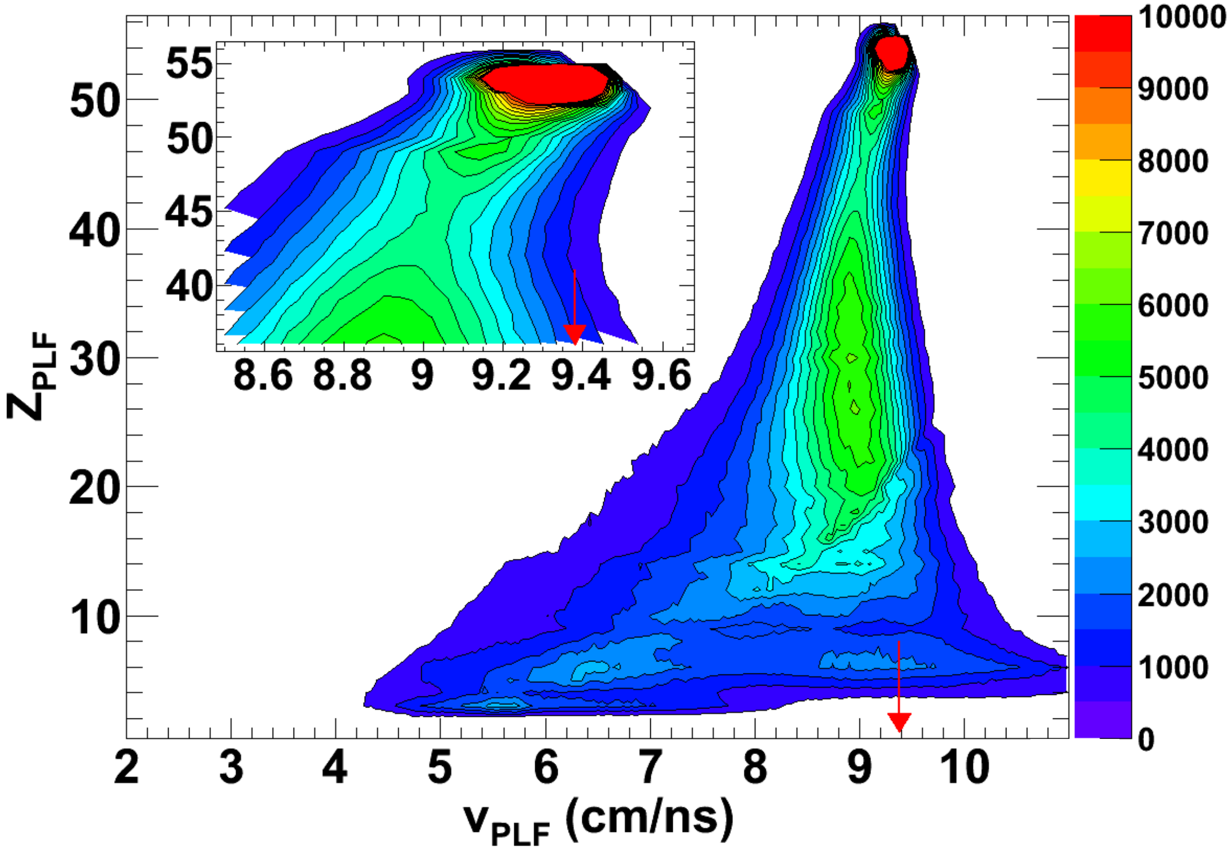

As Z_{PLF} decreases:

- Mean velocity decreases monotonically
- Peak velocity decreases down to ~8.9 cm/ns then rises slightly.

→ Something more than a dissipative PLF-TLF interaction (e.g. dynamic breakup of PLF)

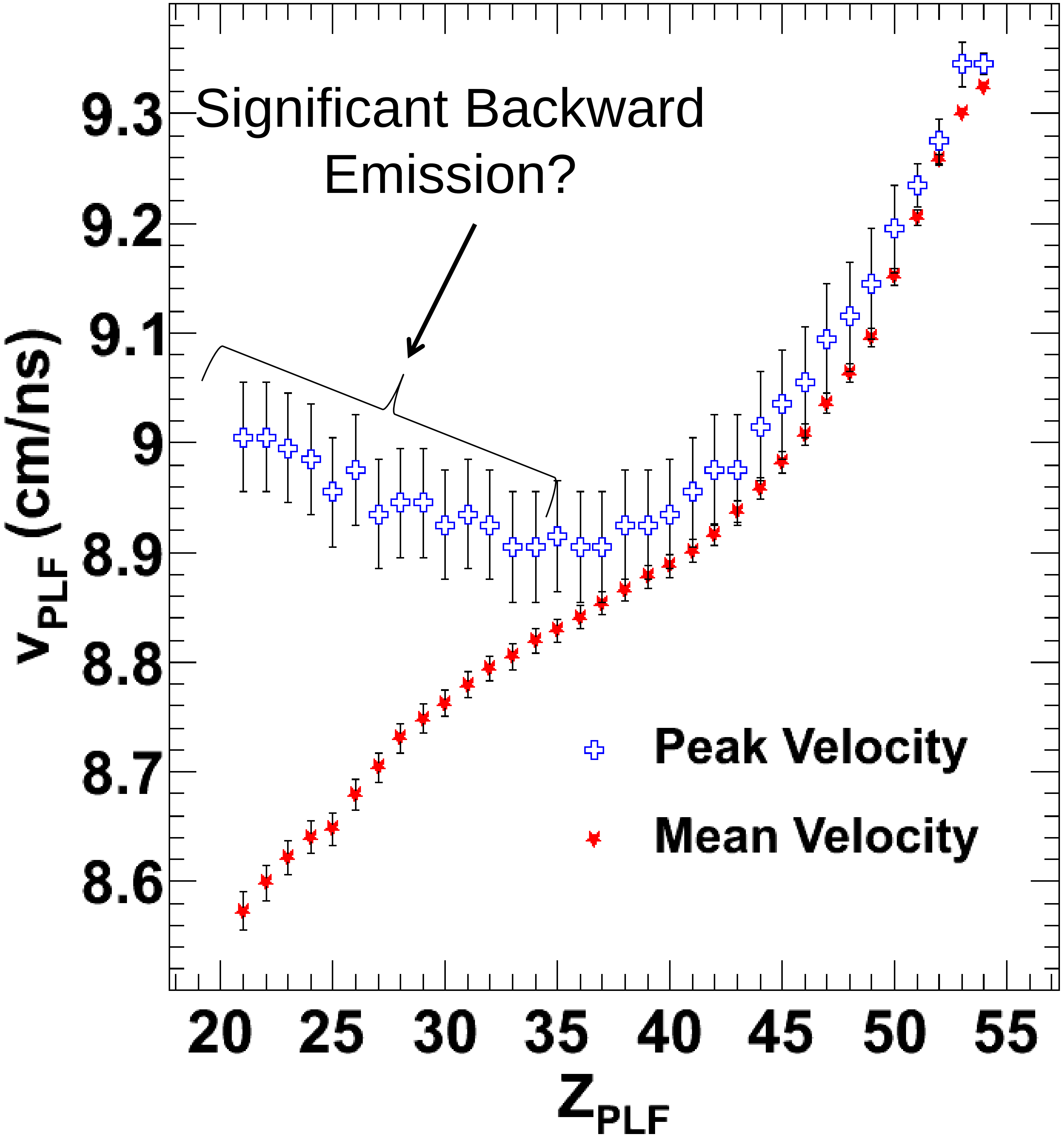

- Two fragments in $3° \leq \theta_{lab} \leq 7°$
- $Z_H \geq 21$
- $Z_L \geq 4$
- $Z_H + Z_L$ at least Z=25 (~ ½ $Z_{projectile}$)

➢ For $Z_L \leq 8$, $V_{parallel}$ distribution for Z_H is single peaked

➢ Associated distribution of $V_{parallel}$ for Z_L has two peaks located at larger and smaller velocities

➢ For $Z_L = 14$ the $V_{parallel}$ distribution for Z_H shows two peaks

Velocity of Z_L is not peaked at the center-of-mass, particularly for heavy Z_L

Consistent with binary decay of a PLF*

$$Z_{PLF*} = Z_H + Z_L$$

$$v_{PLF*} = v_{cm}$$

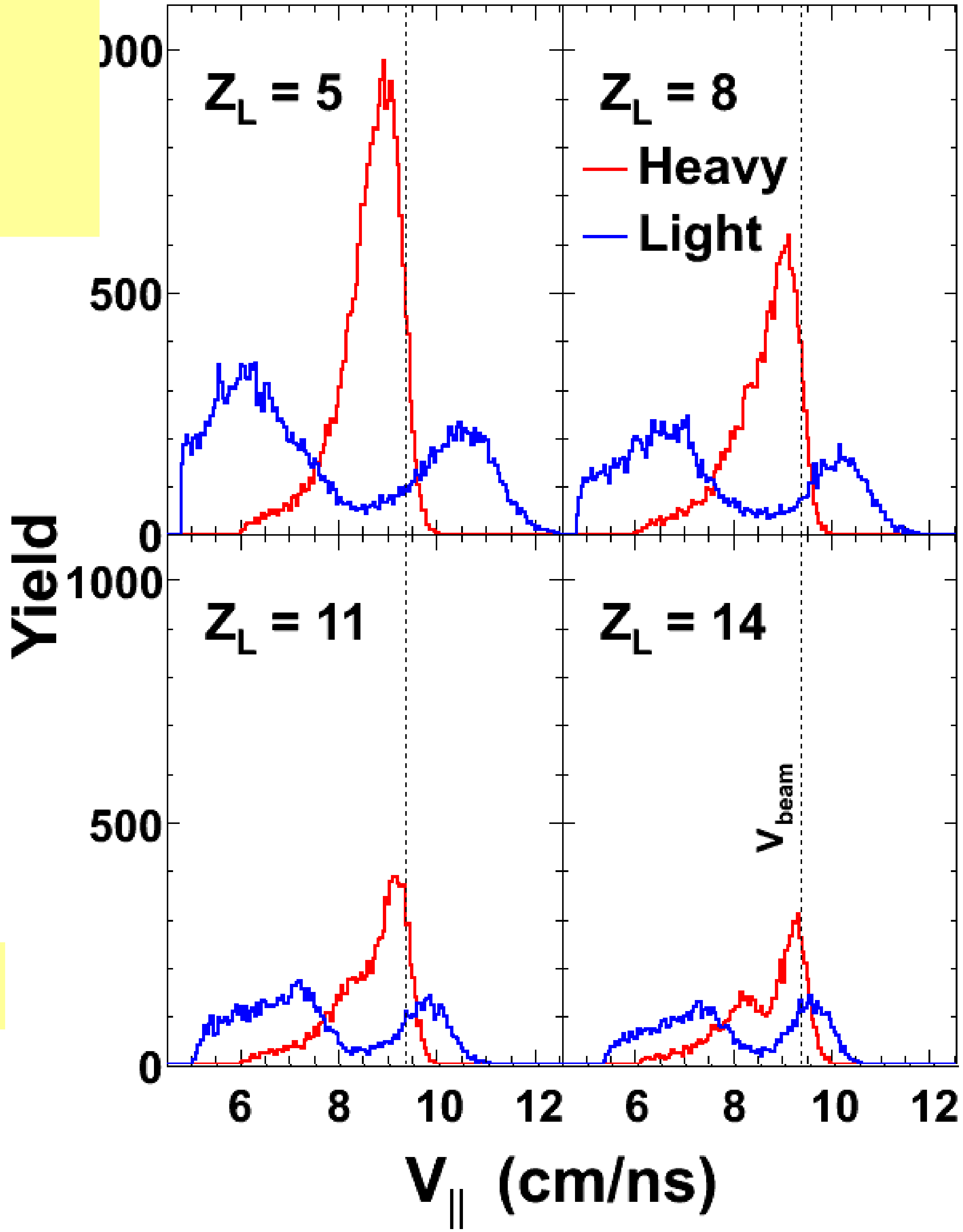

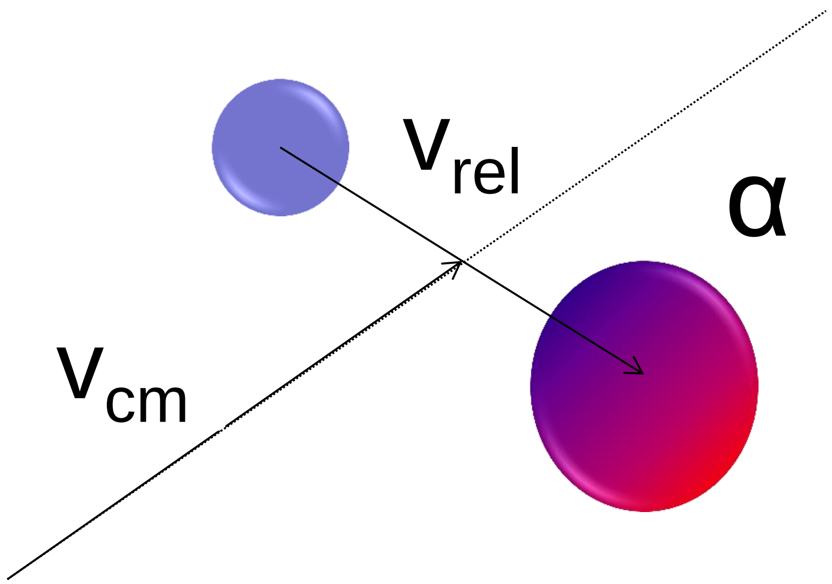

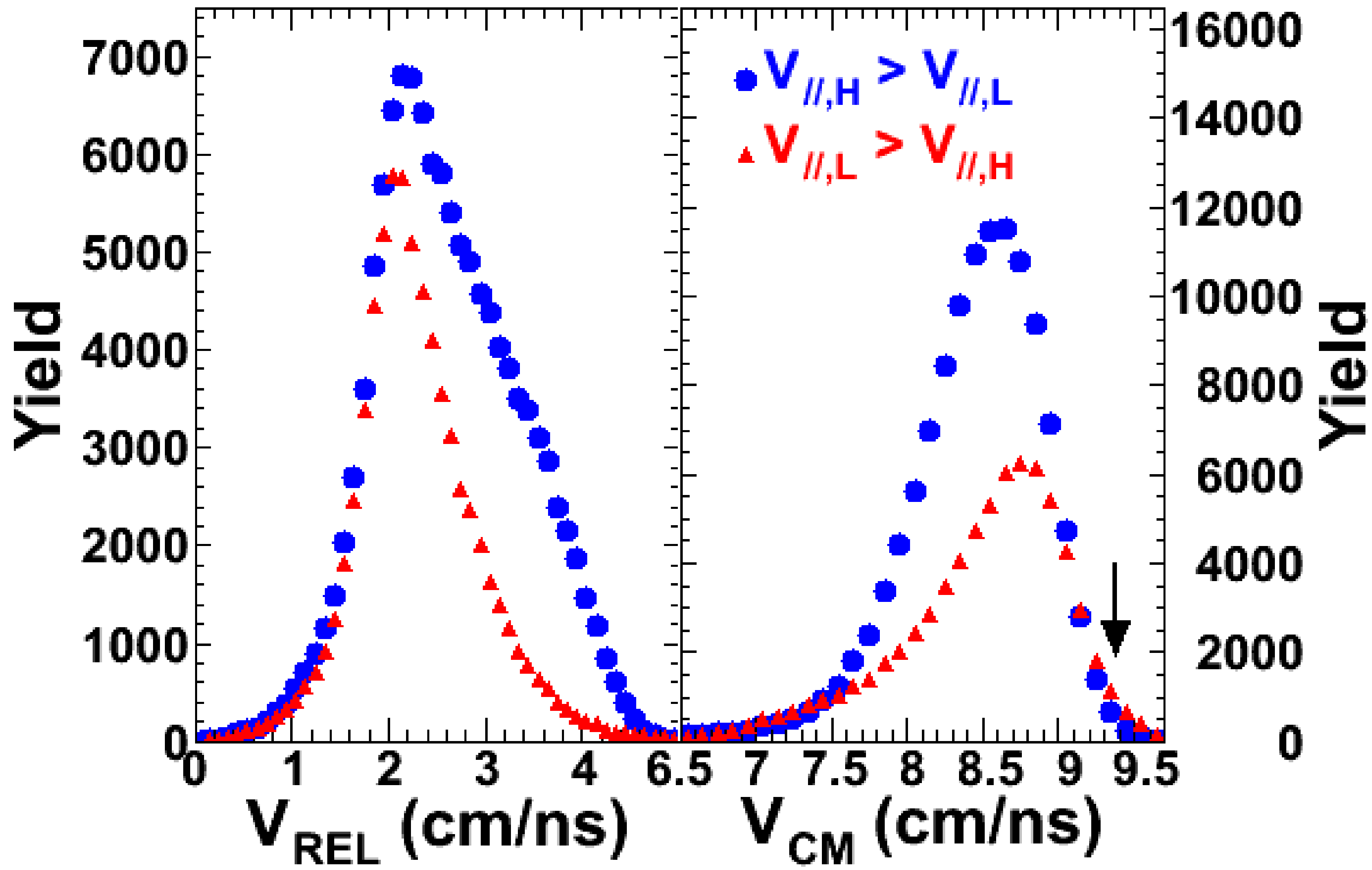

- V_{cm} distributions for $V_H > V_L$ ("**backward emission**") and $V_L > V_H$ ("**forward emission**") are similar, exhibiting damping from beam velocity.
- **Backward emission** has a slightly larger damping on average than **forward emission**.
- **Backward emission** has an additional component of higher relative velocities not observed for **forward emission** (not just mid-rapidity emission).

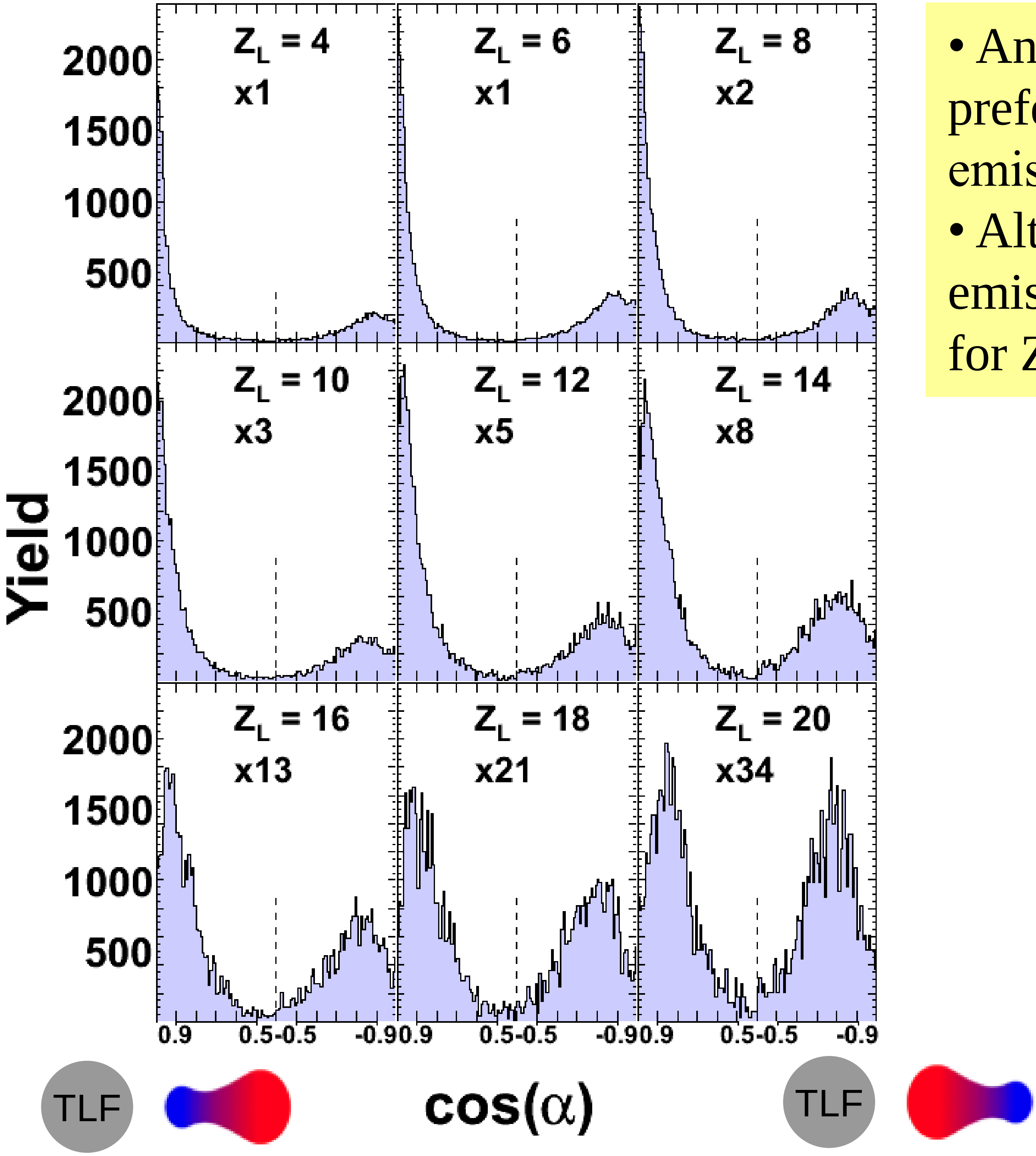

- Angular distribution of the binary decay is preferentially peaked for $\cos(\alpha) > 0$, "backward emission"
- Although asymmetry of forward and backward emission decreases with increasing Z_L, it is still evident for $Z_L = 18$.

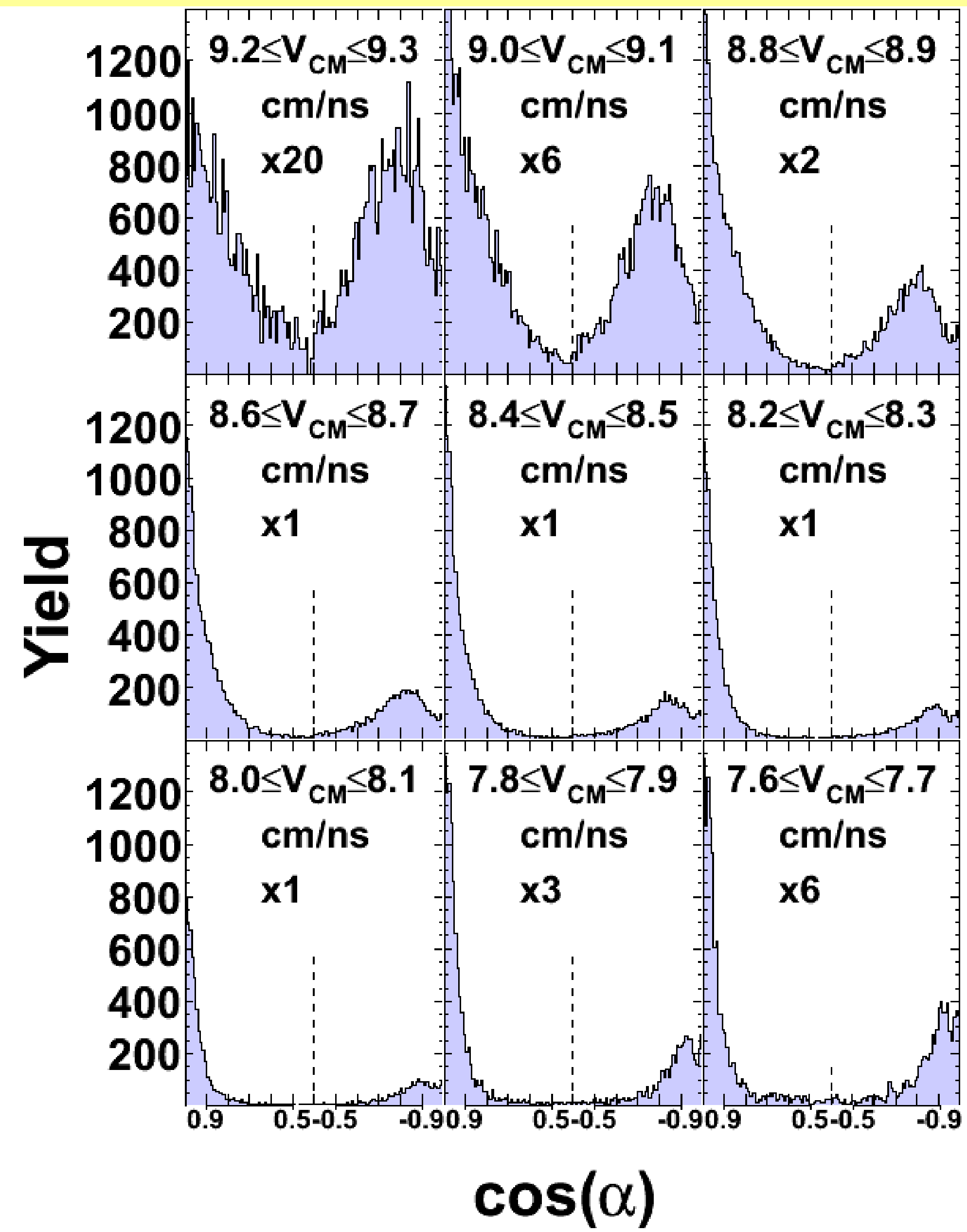

- For the least damped cases, no forward backward asymmetry is evident.
- With increasing damping, the preference for backward emission increases.

McIntosh, PRC81, 034603 (2010)

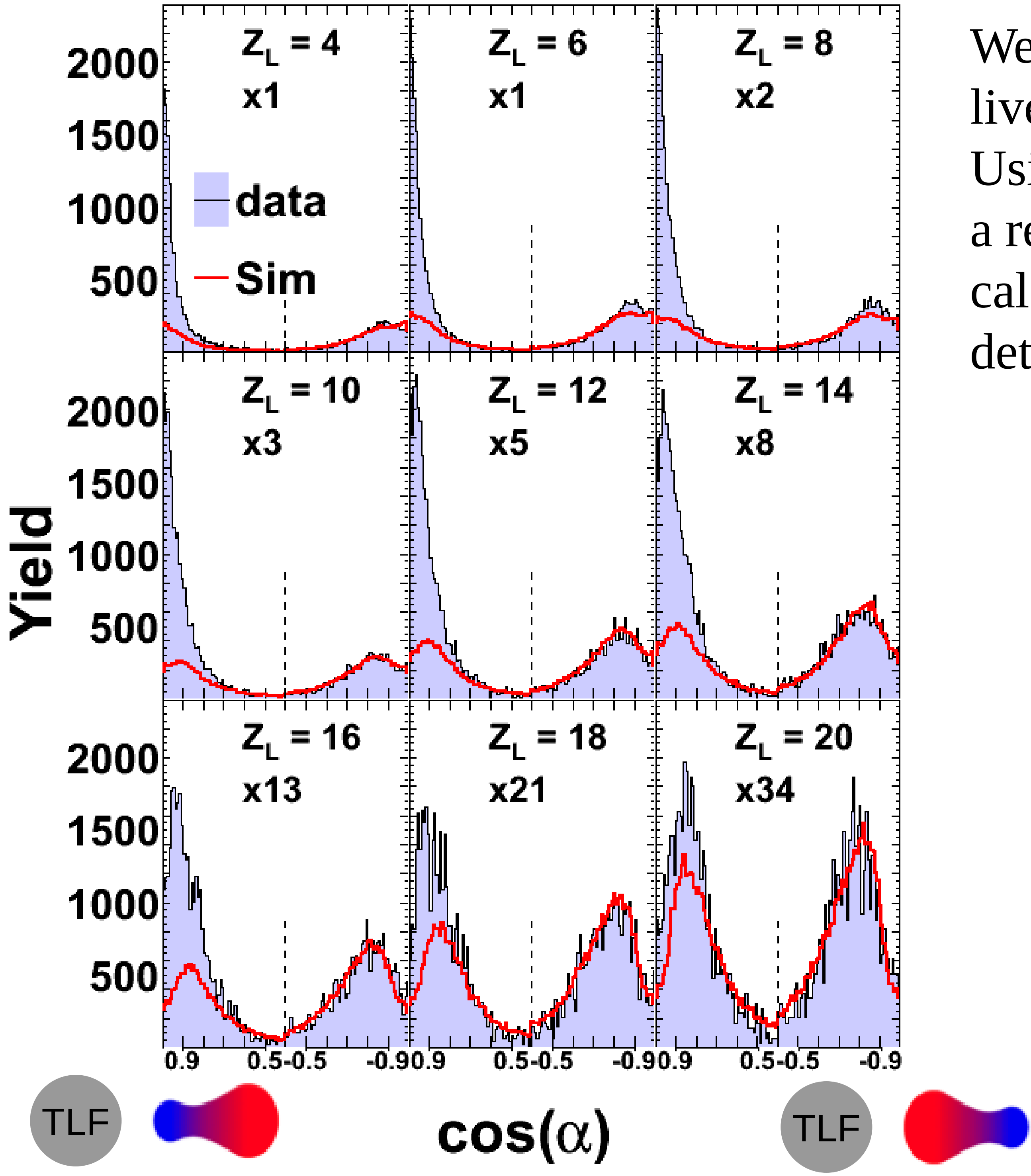

We associate the forward emission with the long-lived statistical emission of a hot, rotating PLF*. Using the observed yield in the forward direction as a reference and assuming isotropic emission, we calculate the backward emission, correcting for the detector acceptance

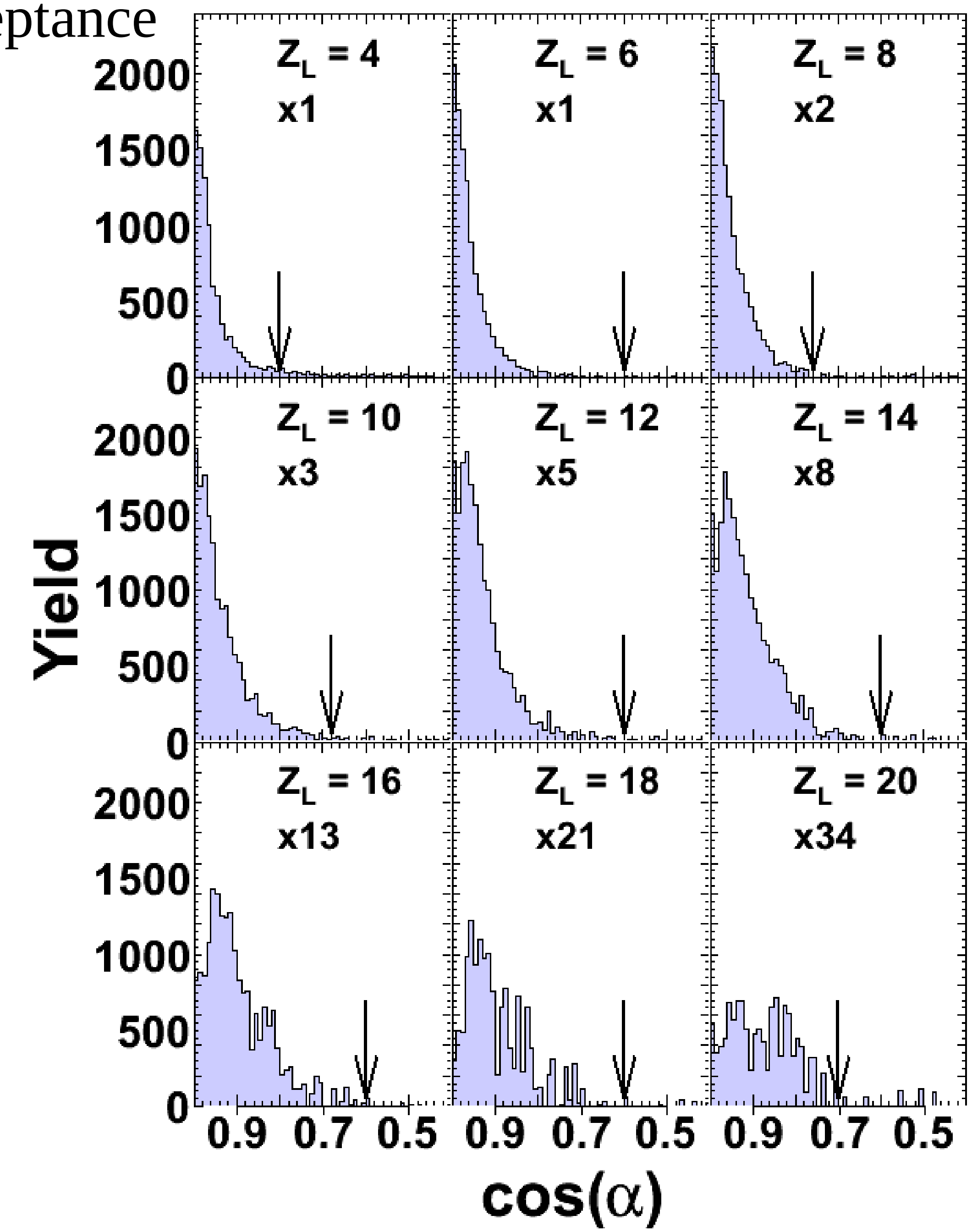

McIntosh, PRC81, 034603 (2010)

The difference distributions reflect the short-lived decays of the PLF*. The angular distributions associated with these decays become broader with increasing Z_L.

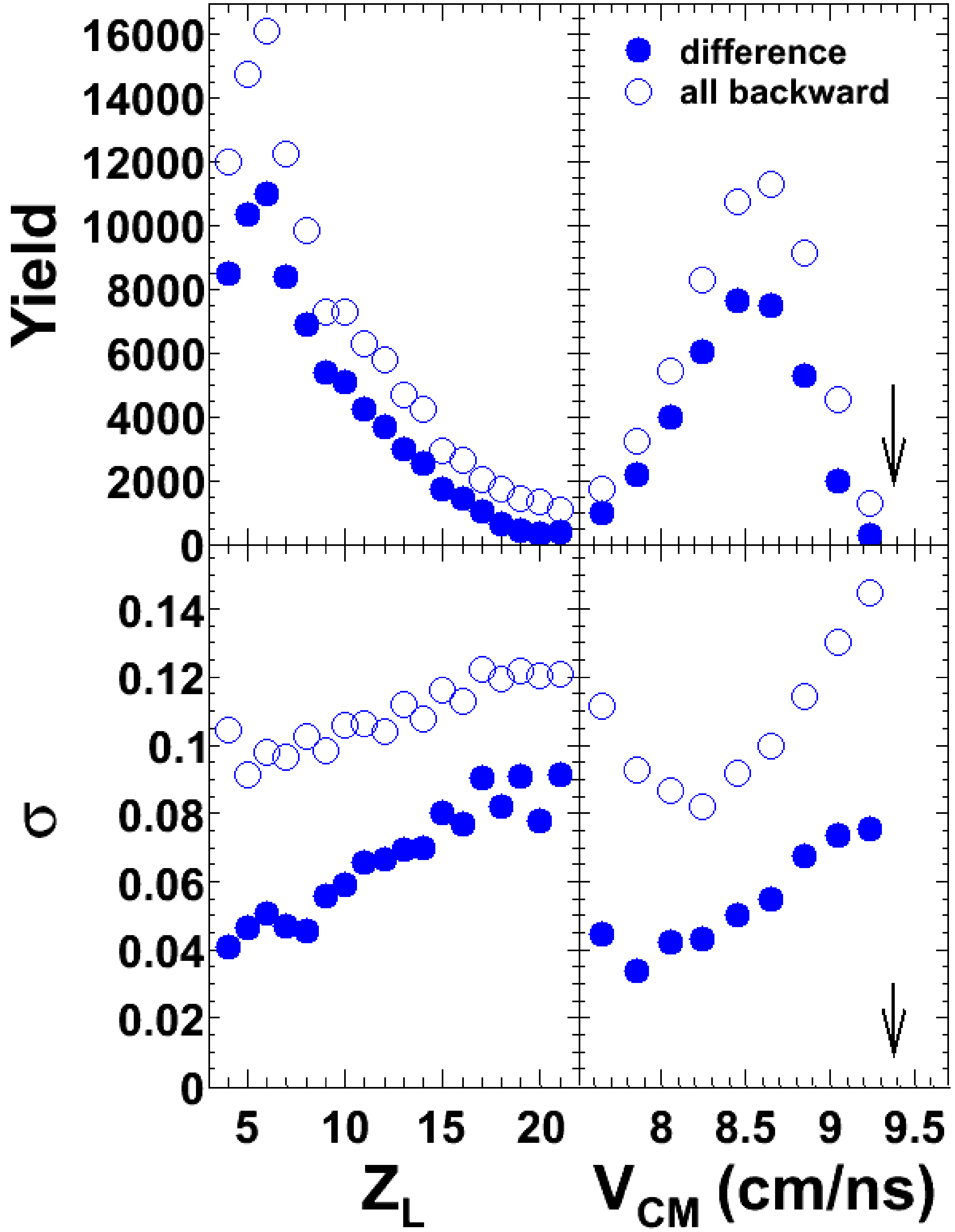

- The yield of the short-lived/dynamical component first increases with increasing Z_L, is peaked at $Z_L = 6$ and then decreases smoothly.

- The distribution of V_{cm} associated with this process is significantly damped from beam velocity.

All major trends observed for the extracted yield (difference) are also observed for the total yield observed backward.

Projectile-Like Dynamical Breakup

- Decay mode characterized by:
  - Strong alignment
  - Large charge asymmetry
  - Preferential emission at velocities intermediate between the projectile and the target
  - Larger relative velocity than standard fission
  - Angular momentum results in rotation

Davin, PRC65, 064614 (2002)
Piantelli, PRL88, 052701 (2002)
Colin, PRC67, 064603 (2003)
McIntosh, PRC81, 034603 (2010)
De Filippo, PRC86, 044605 (2012)

Dynamical fission with multi-neck ruptures

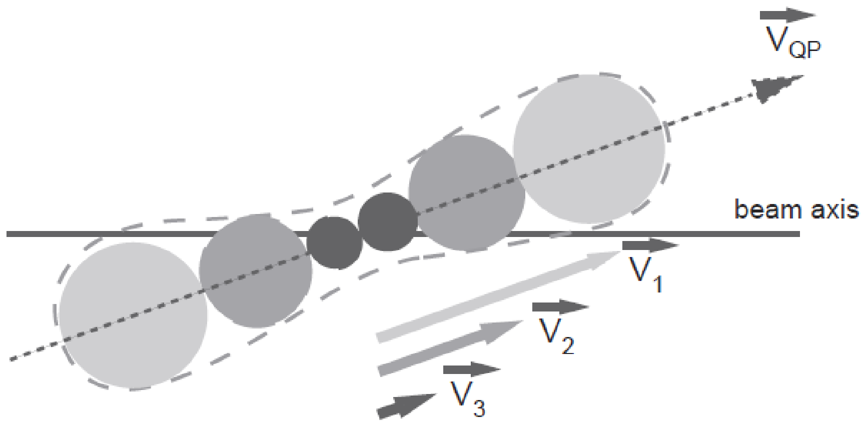

- Relatively long lifetime
  - Much larger than 100 fm/c, the projectile-target contact time

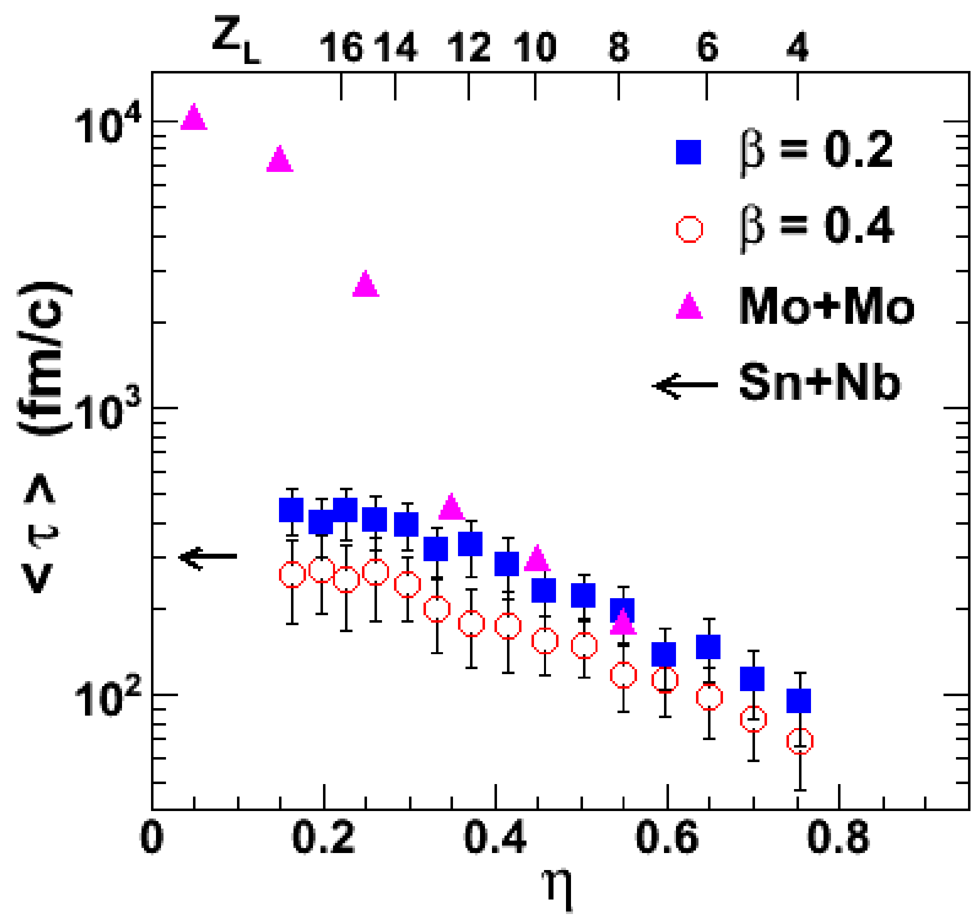

Summary on Binary decay

- **Since Rotation (decay) angle represents time it is a fundamental observable:**

Angle between the relative velocity and the fragment "parent" velocity

- $\cos(\alpha) = 1$: Z_L "backward" of Z_H
- $\cos(\alpha) = -1$: Z_L "forward" of Z_H

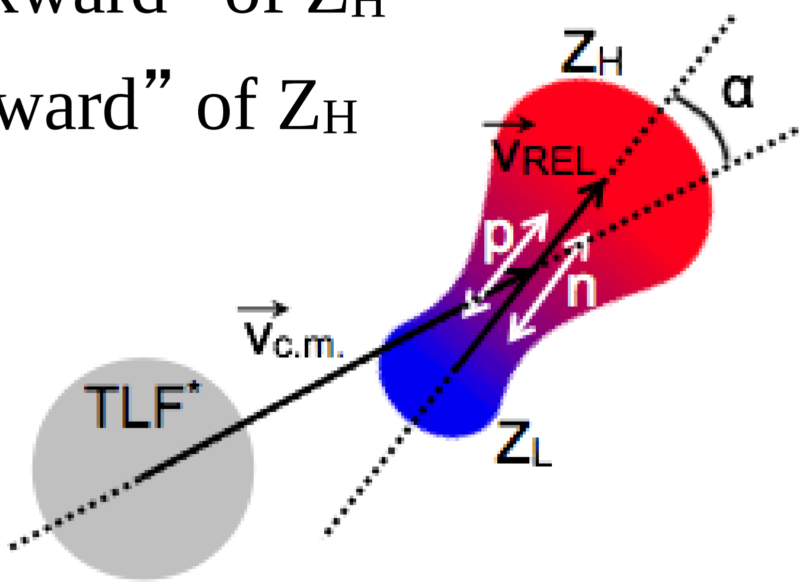

Light fragment **not** emitted at mid-rapidity.

Now examine isotopic composition of Z_L as a function of rotation angle

Event Selection:
1) 2 fragments detected at forward angles: Z_L and Z_H
2) Large fraction of projectile: $Z_H \geq 0.4 * Z_{Projectile}$

McIntosh, PRC81, 034603 (2010)
Hudan, PRC86, 021603(R) (2012)
Brown, PRC87, 061601(R) (2013)

Isotopic Composition vs Rotation Angle

^{124}Xe + Sn

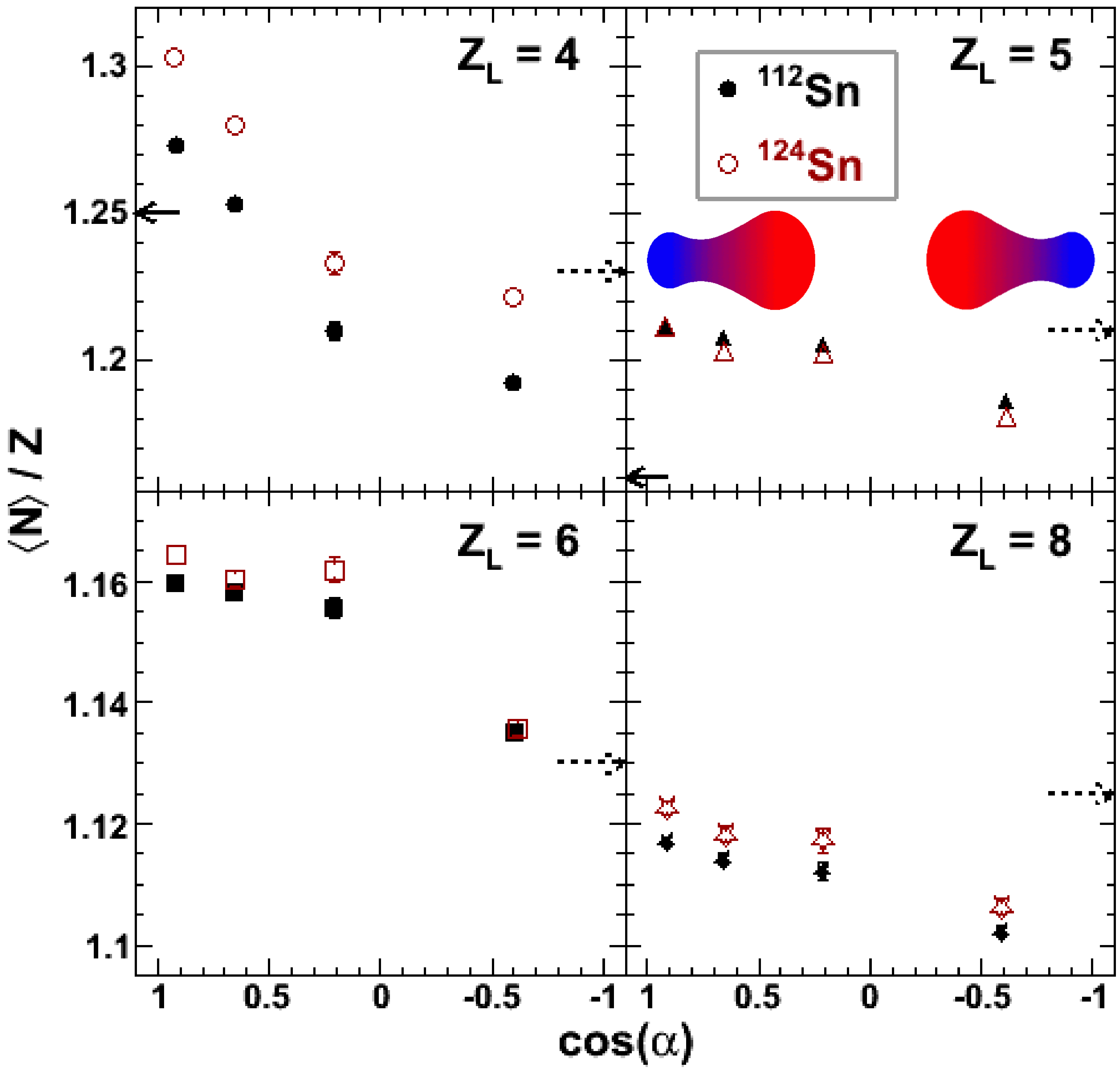

- Backward emission neutron-rich relative to forward emission
- Fragment neutron content enhanced for larger alignment
- Small target effect on the relative neutron composition
- Similar ⟨N⟩/Z observed in ^{124}Sn fragmentation @ 600 MeV/A*

	^{124}Xe	^{124}Sn	^{112}Sn
N/Z	1.30	1.48	1.24

Isotopic Composition vs Rotation Angle

$^{64}Zn + ^{64}Zn, ^{209}Bi, ^{27}Al$

- ⟨N⟩/Z dependence on decay angle for a given Z_L
  - Backward decay neutron-rich relative to forward decay
  - Fragment neutron content enhanced for larger alignment
  - Larger ⟨N⟩/Z values for the Bi target
  - Stronger effect observed for Be fragments

→ "Amplification" of the extremes by the "missing ^{8}Be"

Brown, PRC87, 061601(R) (2013)

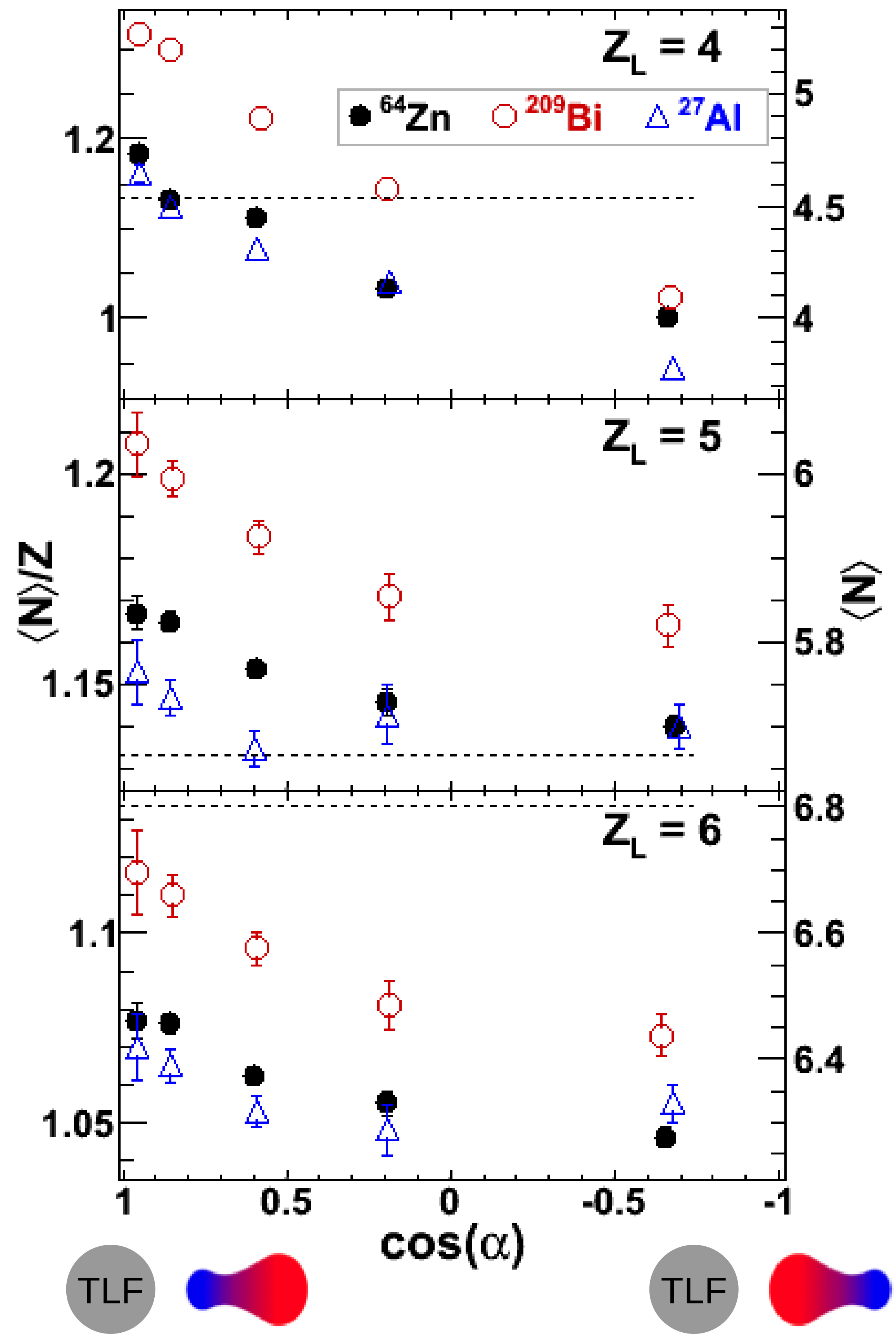

Relating Decay Angle to Time

- The rotation angle can be related to time via the rotational frequency ω:

$$t = \frac{\alpha}{\omega} \quad with \quad \omega = \frac{J\hbar}{I_{eff}}$$

- The angular momentum, J, is determined by the use of a standard statistical emission code to mimic the case of "forward" decay ⇒ J = 6 ± 1 $\hbar$
  - The value of J is *independently* confirmed by α particle's out-of-plane distribution.

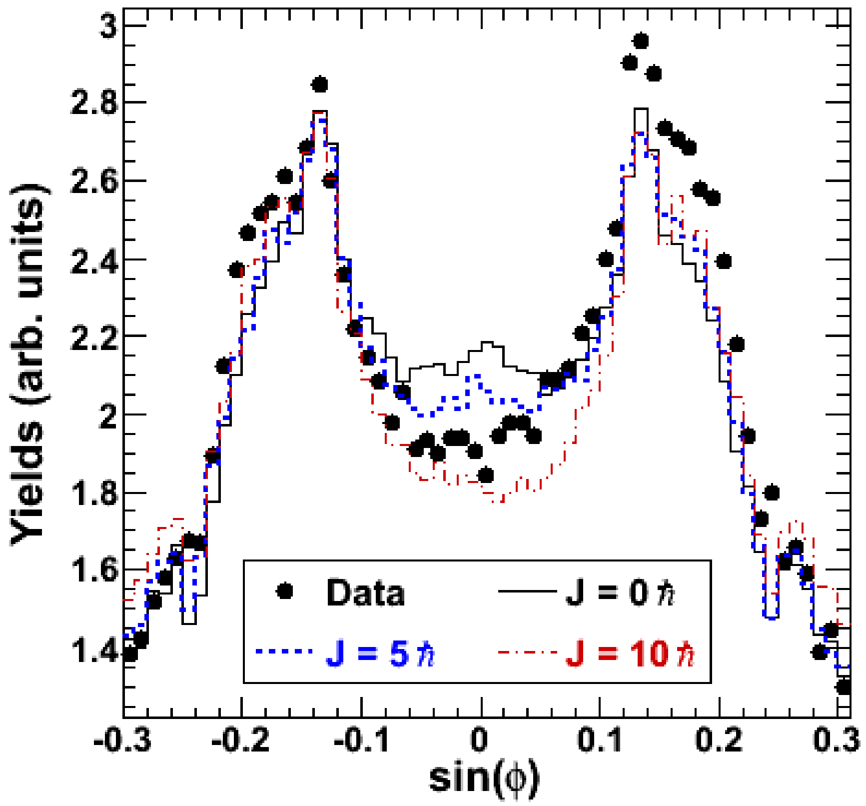

- The moment of inertia, I_{eff}, is calculated for a non-spherical dinuclear shape [Carjan, PRC45, 2185 (1992)] and a temperature T = 3-5 MeV

⇨ $\omega = 0.4\text{-}0.5\times10^{21}$ rad/s

Consistent with previous data
Casini, PRL71, 2567 (1993)
Piantelli, PRL88, 052701 (2002)

Brown, PRC87, 061601(R) (2013)

N/Z Equilibration Timescale

$$\boxed{\Delta\langle N\rangle = \langle N(t)\rangle - N(t=0)}$$

No rotation ⇔ t = 0

cos(α) → time

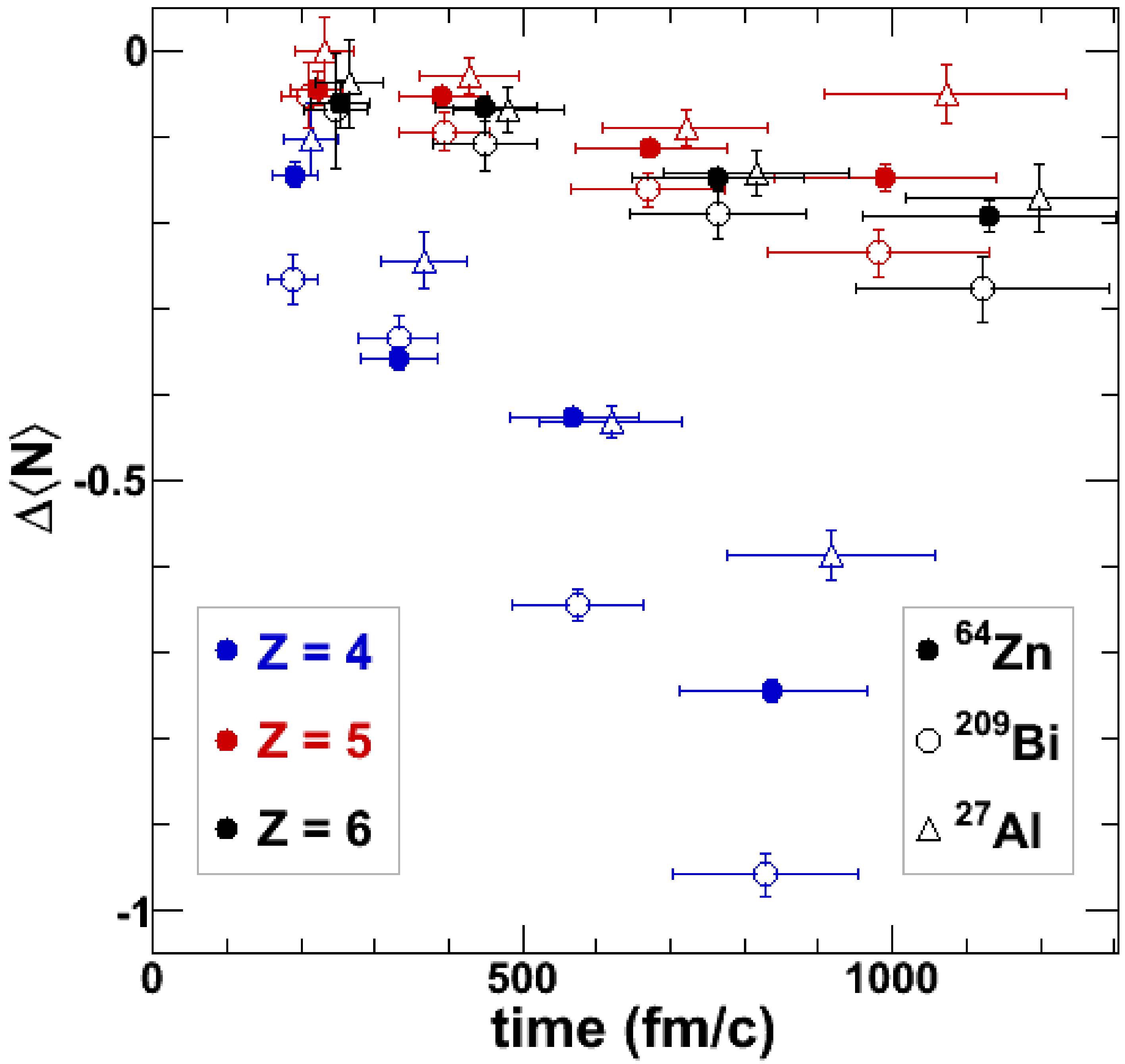

Brown, PRC87, 061601(R) (2013)

- Neutron number of Z_L changes for times as long as 1000 fm/c
- Stronger dependence for $Z_L = 4$
- Target dependence with the strongest slope for the most neutron-rich target
  - Equilibration rate of <N> governed by the initial N/Z gradient in the dinuclear system

N/Z Symmetric Collision

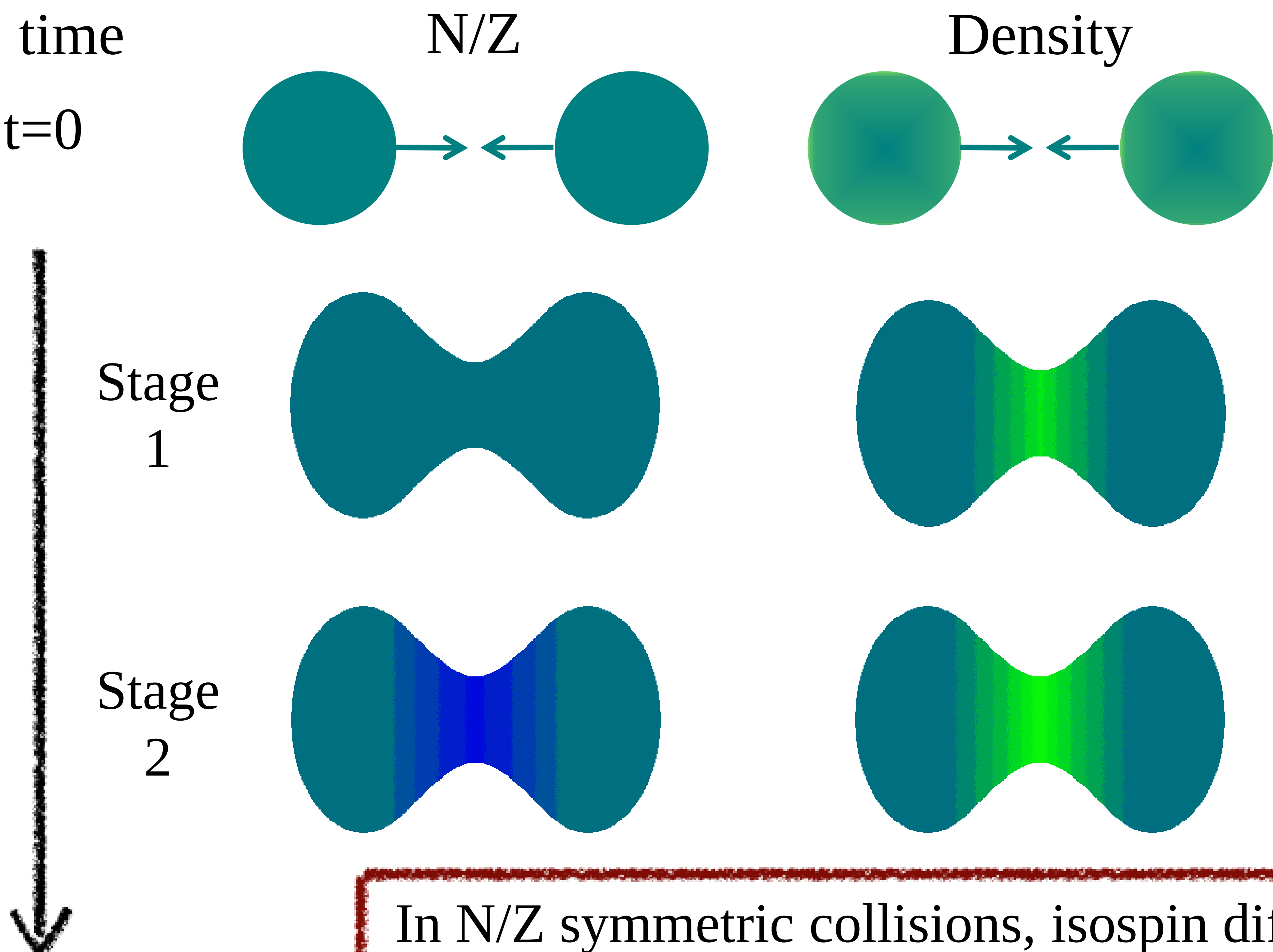

Isospin drift acts to make low density region neutron rich.

Isospin diffusion acts to make the system homogeneous in isospin.

In N/Z symmetric collisions, isospin diffusion would NOT occur without prior isospin drift.

Isospin Drift and Diffusion Timescales

$^{64}Zn+^{64}Zn$ @ 45 MeV/A

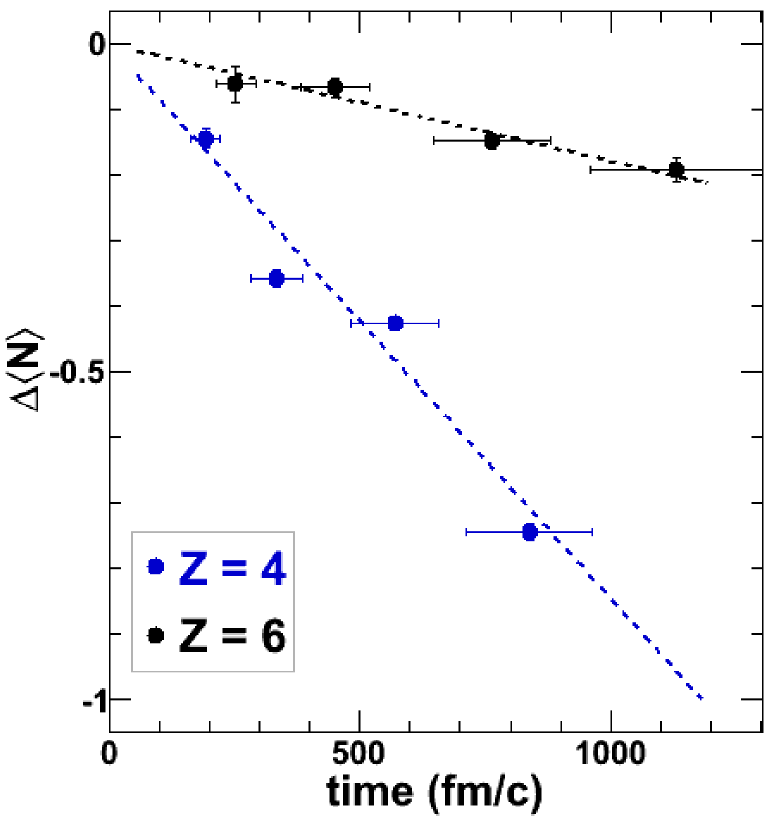

- Isospin diffusion occurs on the timescale of up to ~1000 fm/c
- The impact of isospin drift has independently been observed as neutron enrichment of low density region.
- Isospin drift occurs on a faster timescale, ≤ 100 fm/c

Thériault,
PRC74, 051602 (2006)

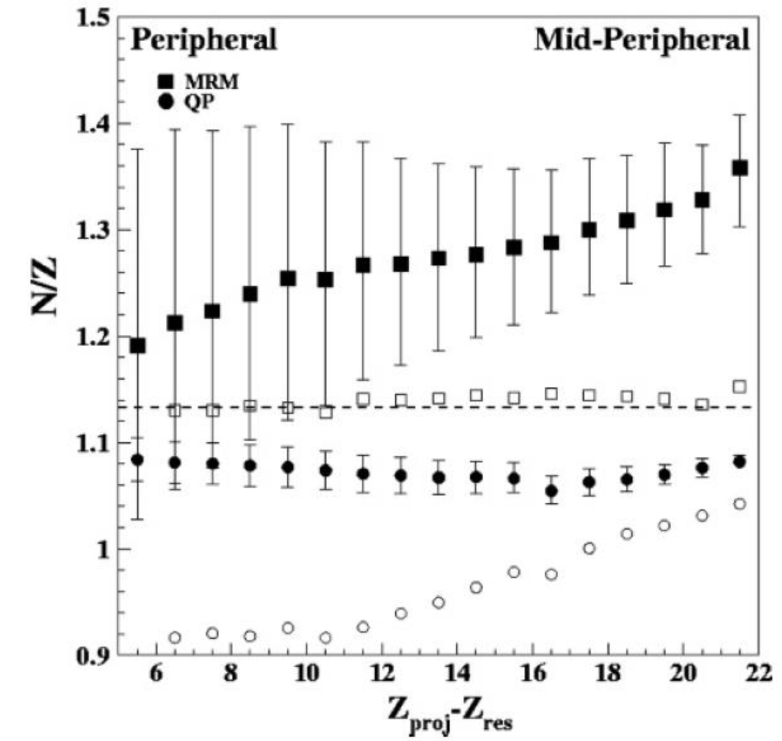

Physical picture

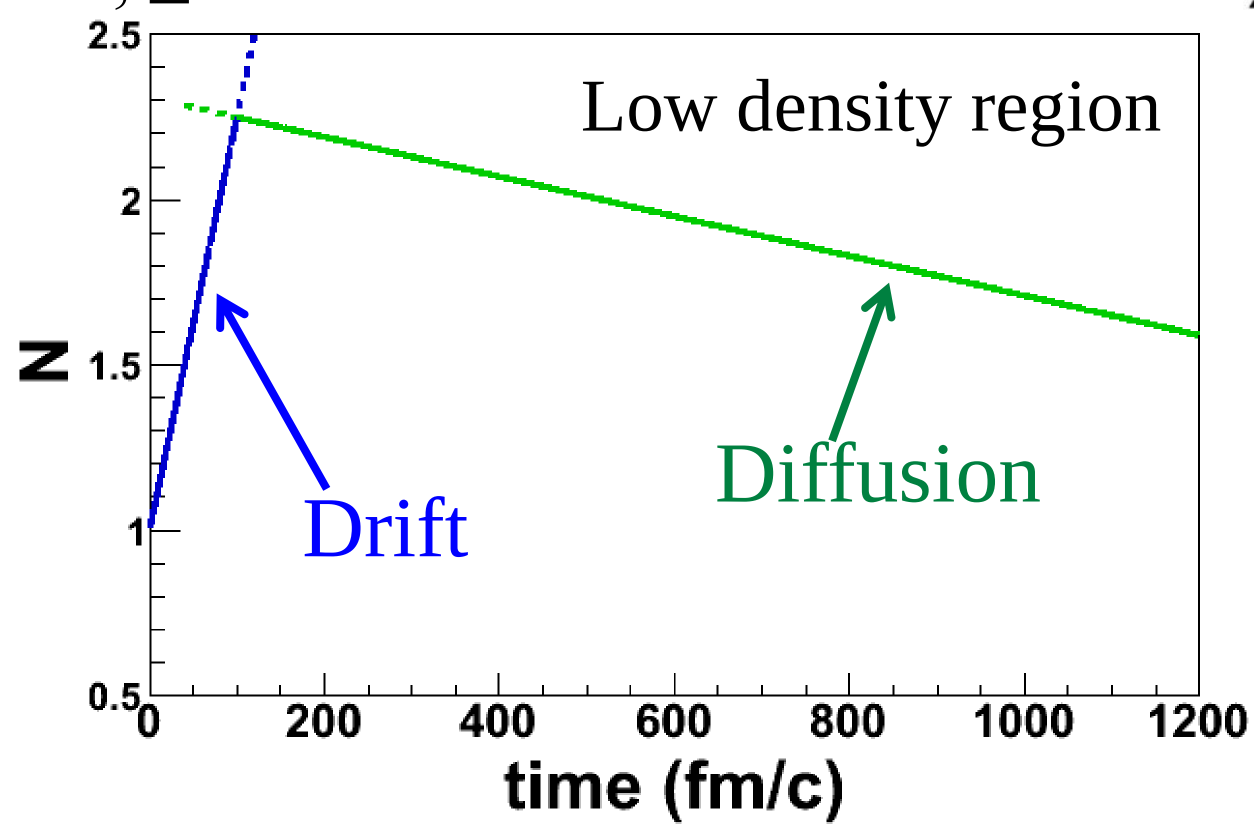

Conclusions

- Dynamical binary decay provides an effective means to access isospin equilibration out to long times t ~ 1000 fm/c

- For symmetric projectile-target combinations, in a first stage drift precedes diffusion establishing an isospin disequilibrium.

- In a second stage, both drift and diffusion contribute in an attempt to return the system to isospin equilibrium with a net flow of neutrons out of the light fragment observed.

- Need microscopic calculations (TDHF ?, *MD?) to better understand this process and relate these observations to

$$\frac{\partial E_{sym}}{\partial \rho} \quad \text{and} \quad E_{sym}$$

Acknowledgements

- Indiana University: A.B. McIntosh, K.W. Brown, J. Black, D. Mercier, C.J. Metelko, B. Davin, R. Yanez, S. Hudan
- GANIL: A. Chbihi
- GSI: S. Bianchin, C. Schwarz, W. Trautmann
- Université Laval, Québec: M.O. Frégeau, J. Gauthier, F. Grenier , J. Moisan, R. Roy, D. Thériault
- Western Michigan University: M. Famiano
- Texas A&M University: S. Yennello's group

Thanks to:

•The support of the GANIL staff and facility

•The support of the Cyclotron Institute at Texas A&M U.

•The DEMON collaboration

This work was supported by the DOE Office of Science under the Grant No. DEFG02-88ER-40404

U.S. DEPARTMENT OF ENERGY

Office of Science